contents were cooled to −25 °C. A suspension of 0.76 g of I_2 (3.0 mmol) in 20 mL of CH_2Cl_2 was added dropwise while the reaction mixture was stirred vigorously. After the addition was complete, the mixture was stirred for 2 h at −25 °C. The CH_2Cl_2 was removed in vacuo. The crude solids were recrystallized from CH_2Cl_2/hexane to give 1.26 g (71%) of ADSbO·I_2 as black needles; mp 220–222 °C. A second crop (0.48 g; 27% of product was recovered from concentration of the mother liquors. First crop ^{1}H NMR: (CD_2Cl_2) δ 1.36 (s, *t*-Bu, 18 H), 8.12 (s, NCH, 2 H). ^{13}C NMR (CD_2Cl_2) δ 26.59 (s, CH_3), 41.25 (s, $C(CH_3)_3$), 121.76 (s, CN), 203.79 (s, CO). ^{14}N NMR (CD_2Cl_2) δ −63. Anal. Calcd for $C_{12}H_{20}NO_2SbI_2 \cdot CH_2Cl_2$: C, 23.26; H, 3.28; N, 2.08. Found: C, 23.08; H, 2.91; N, 1.99.

X-ray Crystal Structure of ADSbO·[MnCp(CO)$_2$]$_2$: Formula, $C_{26}H_{30}NO_6SbMn_2$ monoclinic; space group *C*2/*c* (No. 15); *a* = 1869.9 (2), *b* = 1559.6 (3), *c* = 945.5 (1) pm; β = 92.47 (1)°; *T* = −70 °C; *Z* = 4; FW = 684.16; D_c = 1.649 g/cm^3; μ(Mo) = 18.85 cm^{-1}. Crystal description: black, parallelopiped (0.20 × 0.15 × 0.30 mm) grown by cooling a CH_2Cl_2/hexane solution of ADSbO·[MnCp(CO)$_2$]$_2$. A total of 4354 reflections were collected, 2.2° ≤ 2θ ≤ 55.0°, on a Enraf-Nonius CAD4 diffractometer with graphite monochromator using MoKα radiation (λ = 71.073 pm). With 1948 unique reflections of intensity greater than 3.0σ, the structure was solved by automated Patterson analysis (PHASE) and standard difference Fourier techniques. All non-hydrogen atoms were refined with anisotropic thermal parameters. All hydrogens were placed in calculated positions. The final *R* factors were *R* = 0.046, R_w = 0.038. The final difference Fourier showed the largest residual density to be 0.47 e/Å^3, near the manganese carbonyl carbon, which is synclinal to the tridentate ligand. Atomic coordinates, bond lengths, bond angles, thermal parameters, and additional details are available in supplementary material.

X-ray Crystal Structure of ADAsO·[MnCp(CO)$_2$]$_2$: formula, $C_{26}H_{30}NO_6AsMN_2$ monoclinic; space group *C*2/*c* (No. 15); *a* = 1827.2 (3). *b* = 1216.0 (3), *c* = 1197.2 (3) pm; β = 90.35 (1)°; *T* = −100 °C; *Z* = 4; FW = 637.33; D_c = 1.591 g/cm^3; μ(Mo) = 21.83 cm^{-1}. Crystal description: black, parallelogram (0.36 × 0.21 × 0.50 mm) grown by cooling a CH_2Cl_2/hexane solution of ADAsO·[MnCp(CO)$_2$]$_2$. A total of 3376 reflections were collected, 4.0° ≤ 2θ ≤ 55.0°, on a Syntex R3 diffractometer with graphite monochromator using Mo Kα radiation (λ = 71.073 pm). With 2507 unique reflections of intensity greater than 3.0σ, the structure was solved by automated Patterson analysis (PHASE) and standard difference Fourier techniques. All non-hydrogen atoms were refined with anisotropic thermal parameters. All hydrogens were placed in calculated positions. The final *R* factors were *R* = 0.025, R_w = 0.029. The final difference Fourier showed the largest residual density to be 0.19 e/Å^3, near the manganese. Atomic coordinates, bond lengths, bond angles, thremal parameters, and additional details are available in supplementary material.

X-ray Crystal Structure of ADPO·MnCp(CO)$_2$: formula, $C_{19}H_{25}NO_4PMn$ triclinic; space group $P\bar{1}$ (No. 2); *a* = 916.7 (1), *b* = 941.5 (3), *c* = 1280.4 (2) pm; α = 91.15 (2)°, β = 103.66 (1)°, γ = 106.15 (2)°; *T* = −70 °C; *Z* = 2; FW = 417.33; D_c = 1.349 g/cm^3; μ(Mo) = 7.14 cm^{-1}. Crystal description: pale yellow, irregular block (0.42 × 0.34 × 0.50 mm) grown by cooling a hexane solution of ADPO·MnCp(CO)$_2$. A total of 3722 reflections were collected, 3.3° ≤ 2θ ≤ 50.0°, on a Enraf-Nonius CAD4 diffractometer with graphite monochromator using MoKα radiation (λ = 71.073 pm). With 2956 unique reflections of intensity greater than 3.0σ, the structure was solved by automated Patterson analysis (PHASE) and standard difference Fourier techniques. All non-hydrogen atoms were refined with anisotropic thermal parameters. All hydrogens were placed in calculated positions and refined. The final *R* factors were *R* = 0.029, R_w = 0.036. The final difference Fourier showed the largest residual density to be 0.32 e/Å^3, near the phosphorus. Atomic coordinates, bond lengths, bond angles, thermal parameters, and additional details are available in supplementary material.

X-ray Crystal Structure of ADSbO·I_2: formula, $C_{12}H_{20}NO_2SbI_2 \cdot CH_2Cl_2$ monoclinic; space group $P2_1/n$ (No. 14); *a* = 1015.7 (4), *b* = 1013.7 (3), *c* = 2107.1 (7) pm; β = 98.05 (1)°; *T* = 23 °C; *Z* = 4; FW = 670.78; D_c = 2.07 g/cm^3; μ (Mo) = 43.92 cm^{-1}. Crystal description: black, trapezoid (0.23 × 0.15 × 0.48 mm) grown by cooling a toluene solution of ADSbO·I_2·(CH_2Cl_2). A total of 4812 reflections were collected, 2.0° ≤ 2θ ≤ 53.0°, on a Enraf-Nonius CAD4 diffractometer with graphite monochromator using MoKα radiation (λ = 71.073 pm). After absorption corrections (DIFABS), there were 3496 unique reflections of intensity greater than 3.0σ. The initial atomic coordinates were taken from a room-temperature structure determination with another crystal. All non-hydrogen atoms were refined with anisotropic thermal parameters. All hydrogens were placed in calculated positions and refined. Anomalous dispersion terms were included for iodine and antimony. The final *R* factors were *R* = 0.027, R_w = 0.027. The final difference Fourier showed the largest residual density to be 0.62 e/Å^3 near one of the iodines. Atomic coordinates, bond lengths, bond angles, thermal parameters, and additional details are available in supplementary material.

Acknowledgment is made to Dr. C. A. Stewart for helpful discussions. The excellent technical assistance of J. E. Feaster, Jr., and H. A. Craig made much of this work possible.

Supplementary Material Available: A complete description of the X-ray crystallographic structure determinations on ADSbO·[MnCp(CO)$_2$]$_2$, ADAsO·[MnCp(CO)$_2$]$_2$, ADPO·MnCp(CO)$_2$, and ADSbO·I_2 including experimental procedures, tables of data, and ORTEP structure drawings (20 pages). Ordering information is given on any current masthead page.

Photochemistry of Dipeptides in Aqueous Solution

Roger R. Hill,* John D. Coyle,† David Birch, Edwin Dawe, Graham E. Jeffs, David Randall, Iwan Stec, and Tessa M. Stevenson

Contribution from the Department of Chemistry, The Open University, Milton Keynes MK7 6AA, United Kingdom. *Received June 26, 1990*

Abstract: The photochemical lability of peptides is poorly understood, largely because of the lack of product data. In the present study, product analyses have been carried out following the photolyses in aqueous solution of selected glycyl dipeptides (Gly-Gly, DL-Ala-Gly, L-Val-Gly, L-Pro-Gly, L-Phe-Gly, and Gly-L-Phe), L-prolyl-L-phenylalanine, and L-phenylalanyl-L-proline. Efficient deamination and decarboxylation of aliphatic dipeptides generate thermal precursors of simple amides in a photoinduced electron-transfer process involving the peptide bond. An analogous pathway in the photodegradation of phenylalanyl peptides suffers competition from other types of reaction.

Proteins play an important but ill-defined role in virtually all photobiological processes and are significant targets in biological photodamage. Absorption of solar radiation by prosthetic pigments or aromatic side chains often initiates chemistry remote from the chromophore, but the part played by peptide bonds in such processes remains obscure. The assumption that it is wholly structural, imposing only order and direction, is questionable given, for example, the ready one-electron reduction of peptide groups[1-3] and

† Present address: Cookson Group plc, Sandy Lane, Yarnton, Oxford OX5 1AF, U.K.

(1) Kayushin, L. P.; Ilyasova, V. P.; Azizova, O. A. *Stud. Biophys.* **1978**, *49*, 187-198.

0002-7863/91/1513-1805$02.50/0

their intrinsic photolability.[4-6] The indirect transfer of energy to the peptide linkage may have controlled chemical consequences in some biological systems that contribute significantly to their functions. Particular interest is attached to the possible role of peptide bonds as a medium through which photoinduced[7-9] and ground-state long-distance electron transfer occurs in proteins.[10-13] Photolysis studies with proteins, however, have shed little light on the extent to which peptide bonds become involved in the chemistry. Physical probes are generally too selective, and where irradiation is followed by hydrolysis, information on primary processes is heavily masked by subsequent conversion.[14,15] Such problems have prompted much investigation of the photochemistry of small peptides.

Early and largely inconclusive product studies[5,16-18] reported the release of ammonia and carbon dioxide from dipeptides and evidence for the formation of decarboxylation products, simple amines, and products derived from side chains. Subsequently, the favored approach has been the observation of transients either by flash photolysis[19-21] or by direct[1,22-24] or spin-trap-mediated[25,26] ESR spectroscopy. Species identified include peptide radical anions,[1] radical cations of side-chain aryl groups,[14,24,27-29] and radicals derived from deamination (**1a**),[26] α-CC cleavage (**1b**),[21]

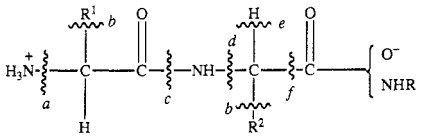

1

peptide bond cleavage (**1c**),[23] secondary deamination (**1d**),[25,26] α-CH cleavage (**1e**),[22,23] and decarboxylation (**1f**).[20,24,25] The relative importance of these intermediates remains unclear, and no general mechanisms have been advanced that accommodate the results satisfactorily. Proposals that the photodegradation of aromatic peptides is initiated by electron transfer from the aromatic ring to the peptide group are well supported, however.[27-29] For example, such a mechanism explains the origin of a cyclization product (**2**) in the photolysis of glycyltryptophan.[29]

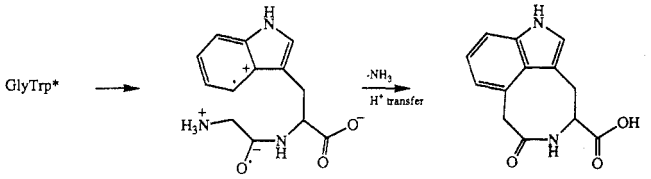

2

The admitted drawback of many of the methods used in the study of peptide photochemistry is that major products arising via intermediates not detectable by the technique employed will be missed. This, and the lack of quantitative data in such product studies as there are, prompted us to attempt comprehensive product analyses following the anoxygenic photolyses of small peptides in aqueous solution.[30-32] In most cases our investigation proceeded in three stages: optimizing conversion for the isolation and estimation of primary nongaseous products using HPLC; isolation and characterization of products using liquid chromatography and spectroscopic methods or GLC interfaced with FTIR spectroscopy; quantitation using HPLC, GLC, gas-sensing electrodes (NH_3), and gravimetric methods (CO_2). Aliphatic dipeptides photolyze cleanly and efficiently to give ammonia (ring opening in prolyl compounds), carbon dioxide, and thermal precursors of amides in good yield. Different product distributions occur at low pH in equally clean reactions. The results are best accommodated by photoinduced intramolecular electron transfer from the carboxylate to the peptide group, followed by deamination, decarboxylation, and formation of a zwitterionic intermediate. Phenylalanyl peptides give a far more complex array of products, but these include, in much lower yield, some of those expected from analogous electron-transfer pathways promoted by excitation in the side chain. Thus, the peptide group participates readily in photoinduced electron-transfer processes.

Experimental Section

General. NMR spectra were recorded with a Bruker WH 400 spectrometer with TMS or DSS as standards, unless stated otherwise. Exact mass measurements were carried out with a VG ZAB-E mass spectrometer and IR spectra were measured with Perkin-Elmer 1310 and FT 1710 spectrometers. UV measurements were made with a Unicam SP8-500 spectrometer. Cation-exchange chromatography and anion-exchange chromatography were performed with Dowex 50-X8 (H^+ form) and Amberlite IRA-401 (formate form), respectively, both supplied by BDH chemicals. Analyses by HPLC were carried out with a Varian 5060 liquid chromatograph. Operating parameters varied a little, but the following were typical: SP, Spherisorb S5 ODS-2, 250 × 5 mm; MP, 10^{-3} M sodium octanesulfonate in 5 × 10^{-3} M KH_2PO_4, pH 2.6; UV detection λ 215 nm. GCFTIR measurements were obtained from a Perkin-Elmer 8410/1700/1710/ system using a 25 m × 0.53 mm i.d. capillary coated to 5-μm thickness with methyl (5% phenyl) silicone bonded phase. GLC analyses were performed on a Pye Unicam 204 chromatograph using a Chromosorb 101 column.

Materials. Dipeptides and other commercial chemicals were purchased from the Sigma Chemical Co. Ltd. or the Aldrich Chemical Co. Ltd. All amino acid residues have L configurations unless indicated otherwise. *N*-(Hydroxymethyl)acetamide,[33] bis(*N*-acetamido)methane,[34] bis(*N*-propanamido)methane,[34] *N*-methyloxamide,[35] glycine methyl-

(2) (a) Baldwin, R. P.; Perone, S. P. *Photochem. Photobiol.* **1977**, *25*, 167-173. (b) Dovgyallo, E. N.; Kuropteva, Z. V.; Pulatova, M. K. *Biofizika* **1978**, *23*, 965-969; *Chem. Abstr.* **1979**, *90*, 99133.
(3) Garrison, W. M. *Chem. Rev.* **1987**, *87*, 381-398.
(4) Weizmann, C.; Hirschberg, Y.; Bergmann, E. *J. Am. Chem. Soc.* **1938**, *60*, 1799-1801.
(5) McLaran, A. D.; Shugar, D. *The Photochemistry of Proteins and Nucleic Acids*; Pergamon: Oxford, U.K., 1964; pp 88-109.
(6) Smith, K. C. In *The Science of Photobiology*; Smith, K. C., Ed.; Plenum: New York, 1989; p 63.
(7) (a) Balzani, V., Ed. *Supramolecular Photochemistry*; NATO ASI Series 214; Reidel: Boston, 1987. (b) Pak, C.; Ishitani, O. *Photochem. Photobiol.* **1988**, *48*, 767-785.
(8) Wasielewski, M. R. In *Photoinduced Electron Transfer*; Fox, M. A., Chanon, M., Eds.; Elsevier: Amsterdam, 1988; Part A, pp 192-199.
(9) Connolly, J. S.; Bolton, J. R. In *Photoinduced Electron Transfer*; Fox, M. A., Chanon, M., Eds.; Elsevier: Amsterdam, 1988; Part D, p 325.
(10) Isied, S. S. *Prog. Inorg. Chem.* **1984**, *32*, 443-517.
(11) Larsson, S. *J. Chem. Soc., Faraday Trans. 2* **1983**, *79*, 1375-1388.
(12) McLendon, G. *Acc. Chem. Res.* **1988**, *21*, 160-167.
(13) Sisido, M.; Tanaka, R.; Inai, Y.; Imanishi, Y. *J. Am. Chem. Soc.* **1989**, *111*, 6790-6796.
(14) Grossweiner, L. I. *Curr. Eye Res.* **1984**, *3*, 137-144.
(15) (a) Schaich, K. M. *CRC Crit. Rev. Food Sci. Nutr.* **1980**, 131-159. (b) Meybeck, A.; Meybeck, J. *Photochem. Photobiol.* **1967**, *6*, 355-363.
(16) Leuschner, G.; Jeschkeit, H.; Losse, G. *Photochem. Photobiol.* **1966**, *5*, 705-719.
(17) Meybeck, A.; Gurtner, B.; Balard, H.; Morvan, R.; Huron, J. L.; Meybeck, J. *Appl. Polym. Symp.* **1971**, *18*, 325-331.
(18) Johns, R. B.; Seurat, M. G. *Photochem. Photobiol.* **1972**, *16*, 413-424.
(19) Chang, M.; Petrich, J. W.; McDonald, D. B.; Fleming, G. R. *J. Am. Chem. Soc.* **1983**, *105*, 3819-3824.
(20) Mittal, L. J.; Mittal, J. P.; Hayon, E. *Photochem. Photobiol.* **1973**, *18*, 281-292.
(21) Bent, D. V.; Hayon, E. *J. Am. Chem. Soc.* **1975**, *97*, 2606-2611.
(22) Meybeck, A.; Windle, J. J. *Photochem. Photobiol.* **1969**, *10*, 1-12.
(23) Neubacher, H.; Schnepel, G. H. *Radiat. Res.* **1977**, *72*, 48-59.
(24) Sevilla, M. D.; D'Arcy, J. B. *J. Phys. Chem.* **1978**, *82*, 338-342.
(25) Lion, Y. F.; Kuwabara, M.; Riesz, P. *J. Phys. Chem.* **1980**, *84*, 3378-3384.
(26) Riesz, P.; Rosenthal, I. *Can. J. Chem.* **1982**, *60*, 1474-1479.
(27) Meybeck, A.; Meybeck, J. *Photochem. Photobiol.* **1972**, *16*, 359-370.
(28) Anderson, J. S.; Bowitch, G. S.; Brewster, R. L. *Biopolymers* **1983**, *22*, 2459-2476.
(29) Dillon, J. *Photochem. Photobiol.* **1981**, *22*, 137-142.
(30) Birch, D.; Coyle, J. D.; Hill, R. R.; Jeffs, G. E.; Randall, D. *J. Chem. Soc., Chem. Commun.* **1984**, 796-797.
(31) Birch, D.; Coyle, J. D.; Hill, R. R.; Jeffs, G. E. *J. Chem. Soc., Chem. Commun.* **1986**, 293-295.
(32) Coyle, J. D.; Hill, R. R.; Jeffs, G. E. *Tetrahedron Lett.* **1987**, *28*, 2529-2532.
(33) Scharf, D. J. *J. Org. Chem.* **1976**, *41*, 28-33.
(34) Gilbert, E. E. *Synthesis* **1972**, *33*, 30-32.
(35) Coyle, J. D.; Hill, R. R.; Randall, D. *Photochem. Photobiol.* **1984**, *40*, 153-159.

amide,[36] *N,N*-diacetylethane-1,2-diamine,[37] *N*-propanoylglycine,[38] 3-benzylpiperazine-2,5-dione,[39] 3-methylbutanoylglycine,[40] *N*,3-dimethylbut-2-enamide,[41] hydrocinnamic acid,[42] and *N*-(3-phenylpropanoyl)-glycine[43] were prepared by known procedures. 3-Methylbutanamide, *N*-(1-oxo-3-phenyl-2-propenyl)glycine,[44] 3-phenylpropanamide, and *N*-methyl-3-phenyl-2-propenamide[45] were prepared by reactions between the appropriate acid chlorides and amines. The methylamides of proline,[46] phenylalanine,[47] and valine[48] and glycine(2-phenylethyl)amide[49] were prepared from the appropriate CBZ-amino acid *p*-nitrophenyl esters and amines by standard methods. *N*-Hydroxymethyl derivatives of propanamide,[50] 3-methylbutanamide, and 3-phenylpropanamide were prepared by Scharf's method.[33] *N*-(Hydroxymethyl)-3-methylbutanamide: cryst ether mp 69 °C; δ_H/ppm ($CDCl_3$) 0.96 (d, 6 H), 2.11 (d, 2 H), 2.30 (m, 1 H), 4.71 (d, 2 H), 4.89 (s, 1 H) 7.1 (b, 1 H); $MH^+ = C_6H_{14}NO_2$ ±<0.1 mmu. *N*-(Hydroxymethyl)-3-phenylpropanamide: cryst water mp, 96 °C; δ_H/ppm DMSO-d_6 2.40 (t, 2 H), 2.85 (t, 2 H), 5.53 (d, 2 H), 5.58 (s, 1 H), 7.23 (s, 5 H) 8.52 (t, 1 H); $MH^+ = C_{10}H_{14}NO_2$ +0.1 mmu.

***N,N'*-Diglycylethane-1,2-diamine (9a).** Ethane-1,2-diamine (0.7 g, 10.9 mmol) was added dropwise to a stirred suspension of CBZ-glycine *p*-nitrophenyl ester (2.7 g, 8.2 mmol) in absolute ethanol (10 mL). The mixture was allowed to stand overnight and the solid product filtered and washed with 1 M sodium hydroxide and water. Drying afforded the crude CBZ derivative of the title compound [0.83 g, 2.0 mmol, 49%, mp 117–118 °C (^{1}H NMR (DMSO-d_6) δ 3.11 (s, 2 H), 3.58 (d, 2 H), 7.35 (s, 5 H), 7.94 (s, 1 H); ^{13}C NMR (DMSO-d_6) δ 41.4, 43.6, 65.3, 127.8, 128.3, 137.0, 156.5, 169.3] which was suspended in glacial acid (2.0 mL) and treated with 30 wt % HBr in acetic acid (1.5 g, 5.6 mmol). After 2 h, the mixture was shaken with dry diethyl ether and the precipitate removed by centrifugation, washed with ether, dissolved in water (5 mL), and extracted with chloroform (3 × 5 mL). The aqueous layer was fractionated by cation exchange (2 × 10 cm) with the eluents water (100 mL), 1 M pyridine (100 mL), and 1 M NH_4OH. The pale yellow oil obtained on evaporation of the last fraction was acidified (5 drops of concentrated HCl) and triturated with absolute ethanol to give a colorless semicrystalline product, spectroscopically and chromatographically identical with that obtained and fully characterized in the photolysis of glycylglycine at pH 1 (below).

***N,N'*-Bis(phenylalanyl)ethane-1,2-diamine (9d)** was prepared from CBZ-phenylalanyl *p*-nitrophenyl ester (1.0 g, 2.4 mmol) by the method used for *N,N'*-diglycylethane-1,2-diamine except that purification by ion-exchange chromatography was omitted. The crude product (0.42 g, 1.2 mmol, 100%) obtained from the final aqueous solution by evaporation was dissolved in the minimum amount of water and the solution adjusted to pH 9 with NaOH. Extraction with dichloromethane and slow evaporation of the extract afforded white crystals: mp 109–110 °C; ^{1}H NMR (D_2O) δ 3.0 (m, 8 H), 4.08 (t, 2 H), 7.30 (s, 10 H); ^{13}C NMR (D_2O) δ 39.1, 40.4, 56.8, 130.2, 131.4, 131.7, 136.1, 171.2. HRMS (CI), $MH^+ = C_{20}H_{27}N_4O_2$ ±<0.1 mmu.

Bis(3-methylbutanamido)methane (6c) was prepared from 3-methylbutanamide and paraformaldehyde by Gilbert's procedure for analogous compounds.[34] The product was recrystallized from tetrahydrofuran: mp 182–185 °C; IR (KBr) 3300, 1645, 1538 cm^{-1}; ^{1}H NMR ($CDCl_3$) δ 0.94 (d, 12 H), 2.04 (d, 4 H), 2.15 (m, 2 H), 4.58 (t, 2 H), 6.88 (b, 2 H). HRMS (CI), $MH^+ = C_{11}H_{23}N_2O_2$ −0.8 mmu.

Photolyses. Except where stated otherwise, photolyses were carried out by one of two procedures. In method A, aqueous solutions of dipeptides (430 mL, 3×10^{-2} M) were degassed and irradiated under argon in a photoreactor (Applied Photophysics) using a 400-W medium-pressure mercury arc located in a centrally placed water-cooled quartz immersion well. In method B, 10–15 mL of degassed aqueous dipeptide solutions (3×10^{-2} M) under argon in each of up to 12 capped quartz tubes were irradiated in a carousel assembly (Applied Photophysics) surrounding the same lamp and immersion well as in method A.

General Procedures. Initial photolyses by method B were monitored by HPLC to establish optimum conversion for primary products. Larger scale photolyses by method A allowed characterization of products by recovery of pure materials, and/or comparisons with standards on the basis of HPLC and GLC behavior, purity parameter measurements in HPLC (diode array detection), and spectra from GCFTIR analyses. Either photolytic method was then used to determine yields of ammonia, carbon dioxide, and less volatile products in solution. Ammonia was determined by ion-selective electrode (Kent Industrial Measurements, 8002-8) and carbon dioxide gravimetrically (via method A) as barium carbonate by Davidson's method.[51] Loss of substrate was measured by HPLC. Multiple analyses under a variety of conditions and purity parameter measurements confirmed peak homogeneity. Quantitative analyses of other components were either by HPLC or GLC as described.

Photolysis of Glycylglycine at pH 6. (a) *N*-Acetylglycine (5a), Acetamide (3a), *N*-(Hydroxymethyl)acetamide (4a), and Bis(acetamido)-methane (6a). Five photolysates, each taken to 35% conversion of substrate by method A (40 h), were combined, evaporated to 200 mL, and continuously extracted for 3 days with dichloromethane. The aqueous fraction was eluted from a cation-exchange column with water to give, after evaporation, 0.96 g of oily crystals. Trituration of a sample with cold, absolute ethanol afforded **5a**. A further sample (0.22 g), dissolved in water (20 mL), was extracted with chloroform (3 × 10 mL), and the gum obtained after drying and evaporating the extract was chromatographed on silica gel to give **4a** (0.12 g) as the principal component. The dichloromethane fraction was dried and evaporated to give crystals (0.4 g). Recrystallization from cold dichloromethane gave acetamide (0.1 g), and chromatography of the remaining solution on silica gel afforded **6a** (0.04 g). Photolysates were analyzed in other experiments for all four products by HPLC using external standards. Acetamide was also monitored by GLC (column temperature 215 °C) with butanamide as internal standard.

(b) Thermal Precursor of Acetamide (7a). After 37% conversion by method A, the photolysate was extracted with dichloromethane for 20 h. The thermally labile component, observed in the aqueous fraction as a well-retained peak by HPLC, was separated by preparative HPLC [Spherisorb S5 ODS2, 2 × (250 × 8 mm); 30 °C; 0.02% aqueous trifluoroacetic acid, 2 mL/min] and obtained as a solution in the eluent (350 mL); 100 mL was heated to boiling for 0.5 h and reanalyzed by HPLC and, for glycylglycine, by TLC (ninhydrin visualization). The solution was treated with standard 2,4-dinitrophenylhydrazine reagent (4 mL) and the yellow solid separated shown to be formaldehyde 2,4-DNP by mp, IR spectroscopy, and HPLC. The remaining 250 mL was lyophilized and analyzed by NMR spectroscopy.

(c) *N*-Methyloxamide and Glyoxylic Acid. Photolysis was carried out by method A to >90% conversion (300 h). Continuous liquid–liquid extraction with dichloromethane (3 days) afforded 74 mg of pale yellow oily crystals from the organic fraction, most of which was acetamide. Trituration with cold chloroform yielded 5 mg of *N*-methyloxamide. Glyoxylic acid in the aqueous fraction was characterized as the ammonium salts of stereoisomeric 2,4-dinitrophenylhydrazones by TLC on cellulose (eluent: butanol/ethanol/1 M ammonium hydroxide 13:2:5) and estimated by HPLC. Thus, 2,4-DNP reagent (0.5 mL) was added to the aqueous fraction (4 mL) and the mixture maintained at 40 °C for 20 min. Ethanol (2 mL) and ethyl acetate (4 mL) were added and, after shaking, the organic layer was washed with 0.5 M HCl (4 mL) and 2 M ammonium hydroxide added (4 mL). After purging with oxygen for 2 min, the aqueous layer was retained for analysis.

(d) Methylamine. In a photolysis by method B, samples were analyzed at increasing conversions of substrate up to 40%. Methylamine was estimated by GLC as its urethane derivative,[52] with the derivative of 1-aminopentane as internal standard.

(e) Quantum Yield for Decomposition. Photolysis was by method B using 1.72 M glycylglycine in the reaction tubes and a 16-W low-pressure mercury arc (Applied Photophysics Model 3016). Other reaction tubes contained, as actinometers, 1,3-dimethyluracil[53] (5.5×10^{-4} M in water)

(36) Marvel, C. S.; Elliot, J. R.; Boettner, F. E.; Yuska, H. *J. Am. Chem. Soc.* **1946**, *68*, 1681–1686.
(37) Clarke, H. J. *A Handbook of Organic Analysis*; Arnold: London, 1926; p 193.
(38) Lee, R. G.; Long, D. A.; Truscott, T. G. *Trans. Faraday Soc.* **1969**, *65*, 820–823.
(39) Frigerio, I. J.; Rae, I. D.; Wong, M. G. *Aust. J. Chem.* **1982**, *35*, 1609–1614.
(40) Tanaka, K.; Isselbacher, K. J. *J. Biol. Chem.* **1967**, *242*, 2966–2972.
(41) Majewski, M.; Mpango, G. B.; Thomas, M. T.; Wu, A.; Snieskus, V. *J. Org. Chem.* **1981**, *46*, 2029–2045.
(42) Ingersoll, A. W. *Organic Syntheses*, 2nd ed.; Gilman, H., Blatt, A. H., Eds.; Wiley: New York, 1967; Collect. Vol. 1, p 311.
(43) Davies, J. S.; Merrit, R. K.; Threadgold, R. C.; Morley, J. S. *J. Chem. Soc., Perkin Trans. 1* **1982**, 2939–2947.
(44) Ronwin, E. *J. Org. Chem.* **1953**, *18*, 1546–1553.
(45) Parkes, E. A.; Polya, J. B.; Spotswood, T. M. *Recl. Trav. Chim. Pays-Bas* **1952**, *71*, 684–688.
(46) Marsh, H. C.; Meinwald, Y. C.; Lee, S.; Martinelli, R. A.; Scheraga, H. A. *Biochemistry* **1985**, *24*, 2806–2812.
(47) Santi, D. V.; Danesberg, P. V. *Biochemistry* **1971**, *10*, 4813–4820.
(48) Poirier, V.; Calleman, C. J. *Acta Chem. Scand. Ser. B* **1983**, *B37*, 817–822.
(49) Essawi, M. Y. H.; Portoghese, P. S. *J. Med. Chem.* **1983**, *26*, 348–352.
(50) Einhorn, A.; Fiebelmann, R.; Gottler, M.; Hamburger, A.; Sprongerts, E. *Liebigs Ann. Chem.* **1908**, *361*, 113–165.
(51) Davidson, R. S.; Goodwin, D.; Platt, J. E. *J. Chem. Soc., Perkin Trans. 2* **1983**, 1729–1733.
(52) Gejvall, T. *J. Chromatogr.* **1974**, *90*, 157–161.

and hexan-2-one[54] (1 M in hexane), and, as a qualitative control to monitor possible concentration effects, 0.03 M glycylglycine. Determination of Φ_{-GG} requires a value for the fraction of light absorbed by the more concentrated substrate solution, which was calculated from ϵ_{GG}^{254} (0.1) and the tube radius (0.5 cm) to be 0.27.

Photolysis of Glycylglycine at pH 1. Photolysis by method A of a solution that had been adjusted to pH 1.0 with perchloric acid was carried out to 74% conversion (11.5 h). Carbon dioxide, ammonia, loss of substrate, and growth of products were monitored at selected intervals by the methods described. The photolysate was reduced to 30 mL by evaporation, and fractionated by cation-exchange chromatography. After no further material was eluted by water (HPLC), 0.1 M pyridine gave 0.33 g of glycylglycine on evaporation. Elution with 1 M ammonium hydroxide afforded, on evaporation, 0.9 g of yellow oil which, dissolved in water (1 mL) and treated with concentrated (HCl (1.5 mL) and ice-cold absolute ethanol (10 mL), yielded, after some solvent evaporation, *N,N'*-diglycylethane-1,2-diamine (**9a**) dihydrochloride (0.15 g): ^{1}H NMR (DMSO-d_6) δ 3.20 (s, 4 H), 3.38 (s, 4 H), 8.27 (s, 6 H); ^{13}C NMR (D_2O) δ 40.8, 42.6, 169.3. HRMS (FAB), (M − 2HCl + H$^+$) = $C_6H_{15}N_4O_2$ ±<0.1 mmu. The filtrate was evaporated and the residue fractionated by anion-exchange chromatography giving glycine methylamide (**8a**) hydrochloride (62 mg) after water elution, evaporation, and treatment with ethanolic HCl. Both products were quantified in photolysates by HPLC.

Comparative Study of Glycylglycine at pH 1, 6, and 12. Three solutions, the first and last adjusted to the required pH with perchloric acid and sodium hydroxide, respectively, were photolyzed by method B. The products were monitored by the methods described.

Photolysis of Glycylglycine in the Solid State. A solution of glycylglycine (2.01 g) in water (20 mL) was evaporated evenly on the inside of a cylindrical quartz vessel [30 × 8 (diameter) cm] with a neck terminating in a 2 cm diameter ground glass joint. The apparatus was flushed with nitrogen throughout irradiation in a Rayonet reactor (Southern New England UV Co., RPR-208) using eight low-pressure mercury arcs (RUL-2537, total output 120 W at 254 nm). Samples were removed periodically for analysis, and the irradiation was terminated ater 239 h, by which time the substrate had become pink. The solid (1.93 g) was dissolved in water (20 mL) and fractionated by cation-exchange chromatography. Elution gave the following components after evaporation: water (250 mL); **5a** (0.10 g); 1 M pyridine (400 mL); glycylglycine (1.68 g); 1 M ammonium hydroxide (300 mL); **8a** (0.17 g).

Photolysis of *N*-Acetylglycine. Irradiation of two tubes of *N*-acetylglycine was carried out by method B. The pH was unadjusted in one tube (2.7) and adjusted in the other to 7.7 with 4 M NaOH. HPLC analysis used a Hypersit ODS column and 2.5 × 10^{-4} M tetrabutylammonium bromide in 10^{-2} M KH_2PO_4 (pH 6.5, λ 220 nm) for *N*-acetylglycine and 10^{-2} M KH_2PO_4 (pH 4.5, λ 215 nm) for *N*-methylacetamide and *N,N'*-diacetylethane-1,2-diamine.

Photolysis of DL-Alanylglycine at pH 6. (a) Propanamide (3b), Bis(propanamido)methane (6b), *N*-(Propanamidomethyl-DL-alanine Methylamide (10b), *N*-Propanoylglycine (5b). Four photolysates obtained by method A (50% conversion; 24 h) were combined, evaporated to 150 mL, and extracted with dichloromethane for 3 days. The aqueous portion was eluted from a cation-exchange column with water, and the crube **5b** obtained (0.4 g) was purified by preparative HPLC [Spherisorb S5 ODS 2, 2 × (250 × 8 mm); 30 °C, H_2O, 2 mL/min] and recrystallization from ethyl acetate. The organic extract was fractionated by normal-phase preparative HPLC (5 μm SiO_2, 250 × 18 mm; 5% CH_3OH in CH_2Cl_2, 2 mL/min; λ 235 nm) from which were isolated **3b** (28 mg), **6b** (140 mg), and **10b** (15 mg): >120 °C dec; ^{1}H NMR (DMSO-d_6) δ 0.97 (t, 3 H), 1.1 (d, 3 H), 2.1 (q, 2 H), 2.4 (b, 1 H), 2.6 (t, 3 H), 3.1 (q, 1 H), 3.7 (dd, 1 H), 3.9 (dd, 1 H), 7.9 (q, 1 H) 8.0 (t, 1 H); ^{13}C NMR (DMSO-d_6) δ 10.6, 20.3, 26.3, 29.4, 53.4, 54.9, 174.5, 175.0. MS (EI); *m/z* 129, 87, 53, 56. **3b** and **5b** were quantified by HPLC, and **3b** was quantified by GLC (Chromosorb 101; 215 °C; butanamide, internal standard).

(b) *N*-(Hydroxymethyl)propanamide (4b). Photolysis by method A was continued to 35% conversion (17 h). After evaporation to 10 mL, the photolysate was eluted from a cation-exchange column with water, evaporated to 10 mL, eluted from an anion-exchange column with water, and evaporated to dryness to give **4b** (0.2 g). Quantitation in other photolyses was by HPLC.

Photolysis of DL-Alanylglycine at pH 1. Photolysis by method A of a solution that had been adjusted to pH 1 with perchloric acid was carried out to 85% conversion (7 h). Fractionation by cation-exchange chromatography with the eluents water (250 mL), 1 M pyridine (400 mL), and 1 M NH_4OH (250 mL) gave, after evaporation of the last fraction, a brown crystalline gum (1.0 g) whose NMR spectra were consistent with a 2:1 molar ratio of DL-alanine methylamide (**8b**) and *N,N'*-dialanylethane-1,2-diamine (**9b**): ^{1}H NMR (D_2O) δ 1.1 (d, 3 H), 3.2 (s, 2 H), 3.35 (q, 1 H); ^{13}C NMR (D_2O) δ, 22.1, 40.9, 52.0, 179.8). Both products were quantified by HPLC.

Photolysis of Valylglycine at pH 6. Photolysis by method A was carried out to 70% conversion (8 h) and, after evaporation to 150 mL, the photolysate was continuously extracted with dichloromethane for 3 days. The organic fraction was dried over anhydrous magnesium sulfate and evaporated to give a pale yellow gum (180 mg). GCFTIR examination ($CHCl_3$ solution, injector temperature 250 °C; oven temperature 170 °C) established the presence of 2-methylbutanamide (**3c**) and valine methylamide (**8c**). Chromatography on silica ($CHCl_3$–$CHCl_3$/CH_3OH 20:1) afforded, as the fifth of nine product fractions, 60 mg of *N*-(3-methylbutanamidomethyl)valine methylamide (**10c**): recrystallized methanol/ether, mp 150 °C; ^{1}H NMR ($CDCl_3$) δ 0.82 (d, 3 H), 0.90 (d, 3 H) 0.92 (d, 6 H), 2.15 (m 4 H) 2.25 (b, 1 H) 2.79, (d, 3 H) 3.56, (dd, 1 H) 4.42 (dd, 1 H), 6.89 (t, 1 H), 7.19 (q, 1 H); ^{13}C NMR ($CDCl_3$) δ 17.6, 19.4, 22.4, 25.6, 25.8, 31.1, 45.7, 53.7, 64.3, 173.8, 174.4. HMRS (CI), MH$^+$ = $C_{12}H_{26}N_3O_2$ +0.3 mmu. The aqueous fraction was applied to a cation-exchange column, and elution with water and evaporation afforded 3-methylbutamide (**3c**) (20 mg). *N*-(Hydroxymethyl)-3-methylbutanamide (**4c**) was established by comparison with the HPLC and temperature-dependent GLC behavior of a synthesized sample. **3c**, **4c**, and **8c** were quantified by HPLC. **3c** and **8c** were also analyzed by GLC (bonded methyl silicone 25 m × 0.53 mm i.d., 5-μm film, 140 °C, butanamide internal standard).

Photolysis of Prolylglycine at pH 6. Photolysis by method A was carried out to 70% conversion (40 h) and the photolysate extracted with dichloromethane for 3 days. The aqueous portion was fractionated by cation-exchange chromatography by eluting with water (250 mL) and 1 M pyridine (500 mL). The latter fraction was evaporated and the residue derivatized with benzyl chloroformate by standard methods. The ethyl acetate extract from basic reaction mixture was separated by normal-phase preparative HPLC (250 × 8 mm, 5 μm SiO_2; 4% CH_3OH in CH_2Cl_2, 2 mL/min; λ 235 nm). The third of four components afforded, after rechromatography, 8 mg of *N,O*-bis-CBZ-5-amino-*N*-(hydroxymethyl)pentanamide (**13a**): mp 76 °C; ^{1}H NMR ($CDCl_3$) δ 1.47 (qnt, 2 H) 1.62 (qnt 2 H), 2.20 (t, 2 H), 3.13 (q, 2 H), 3.99 (d, 2 H), 4.82 (t 1 H), 5.02 (s, 2 H), 5.11 (s, 2 H), 5.99 (t, 1 H) 7.28 (m 10 H); decoupling experiments established related signals; ^{13}C NMR ($CDCl_3$) δ 22.3, 29.2, 35.4, 40.3, 41.2, 66.5, 67.1, 128.0, 128.3, 128.4, 128.45, 128.55, 136.5, 156.4, 160.8; IR (KBr) 3324, 1736, 1683, 1658, 1532 cm^{-1}. HRMS (EI), no M$^+$ but M − ($C_6H_5CH_2O$) − CO_2 = $C_9H_{15}N_3O_3$ ±<0.1 mmu, and other ions expected for CBZ derivatives.[32] **13a** (1.7 mg) was hydrogenolyzed for 24 h in formic acid (0.2 mL), methanol, and water (0.4 mL) over Pd on PEI polymer beads [Pierce (U.K.) Ltd.] (28 mg) and the product mixture analyzed by HPLC and GCFTIR. 2-Piperidone was quantified in fresh photolysate by GLC using the conditions described for GCFTIR earlier.

Photolysis of Prolylglycine at pH 1. Photolysis by method B of 100 mL of a solution that had been adjusted to pH 1.25 with HCl and distributed among eight tubes was carried out to 60% conversion (60 h). The photolysate was fractionated by preparative HPLC (SP, Spherisorb S5 ODS-2, 250 × 8 mm; MP, 0.01 M TFA in 2% acetonitrile; λ 215 nm; FR, 2.5 mL/min; sample, 300 × 0.3 mL) and the most highly retained peak collected. Evaporation afforded 40 mg of **9e** bis-TFA salt: ^{1}H NMR (D_2O) δ 1.95 (m, 6 H), 2.35 (m, 2 H), 3.3 (m, 8 H), 4.25 (t, 2 H); ^{13}C NMR (D_2O) δ 24.2, 30.0, 39.3, 46.9, 60.3, 163.2 (q), 170.1, 191.2. HRMS (FAB), MH$^+$ = $C_{12}H_{23}N_4O_2$ +0.1 mmu.

Carbon dioxide was determined in a separate photolysis by method A.

Photolysis of Phenylalanylglycine at pH 6. (a) 3-Phenylpropanamide (3d), *N*-(Hydroxymethyl)-3-phenylpropanamide (4d), Phenylalanine Methylamide (8d), and Glycine. Half of the photolysate obtained by method A after 40% conversion (32 h) was extracted manually with chloroform. Evaporation gave a pale yellow gum (62 mg) that was analyzed by GCFTIR directly (establishing **3d**) and after silylation with bis-TMS acetamide (establishing **3d**, **4d**, and **8d**). All but glycine were quantified by HPLC, and 3-phenylpropanamide was also analyzed by capillary GLC (bonded methyl silicone, 25 m × 0.53 mm i.d., 5-μm film; 200 °C, benzamide internal standard). Glycine was estimated by GLC of its derivative with BSTFA formed by standard procedures with a lyophilized sample of the photolysate.

(b) Quantum Yield for Decomposition. Photolysis by method B incorporated 1,3-dimethyluracil as an actinometer.

Photolysis of Phenylalanylglycine at pH 1. Photolysis by method A of a solution that had been adjusted to pH 1.3 with acid was carried out to 20% conversion (2 h). The photolysate was extracted with dichloro-

(53) Nuamo, N.; Hamanda, T.; Yonemitsu, O. *Tetrahedron Lett.* **1977**, *19*, 1661–1664.

(54) Murov, S. L. *Handbook of Photochemistry*; Dekker: New York, 1973; p 126.

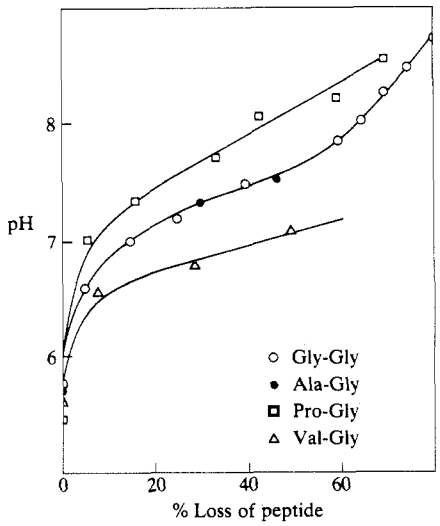

Figure 1. Changes in pH during photolysis of aqueous dipeptides by method A.

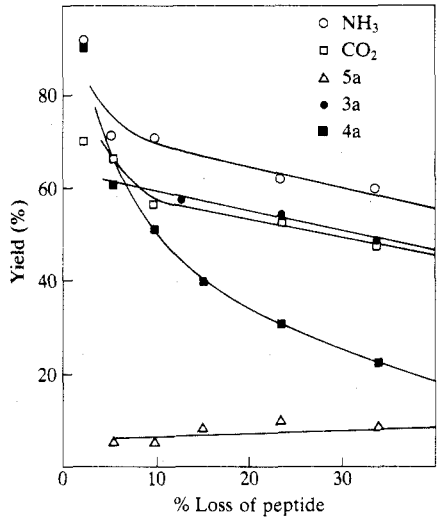

Figure 2. Yield profiles for major products in the photolysis of glycylglycine in neutral aqueous solution.

methane for 5 days, and the aqueous layer was removed, adjusted to pH 12 with sodium hydroxide, and extracted with dichloromethane for a further 5 days. Evaporation of the last organic fraction afforded **8d** (57 mg).

Photolysis of phenylalanine methylamide (8d) at pH 1 was carried out by method B.

Photolyses of Prolylphenylalanine and Phenylalanylproline at pH 6. Solubility limited photolysis of prolylphenylalanine to 4×10^{-3} M solution. Otherwise, general procedures were applied. 2-Piperidone was quantified in prolylphenylalanine photolysis as in the photolysis of prolylglycine.

Results

Glycylglycine. Irradiation of 0.03 M aqueous glycylglycine to >90% reaction yields acetamide (~15%) as the principal isolable product, almost certainly derived from secondary reactions. Moreover, photolysis is accompanied by an increase in pH (Figure 1), and it was desirable to retain the substrate in one conjugate form without the assistance of buffers. Typically, photolyses of initially near neutral aqueous glycylglycine were taken to 30–50% conversion, from which were obtained, by liquid extraction and chromatography, acetamide (**3a**), *N*-(hydroxymethyl)acetamide (**4a**), *N*-acetylglycine (**5a**), and *bis*(acetamido)methane (**6a**). All

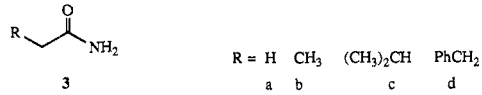

3

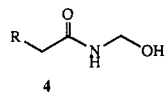

4

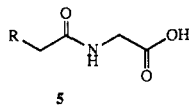

5

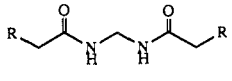

6

but **6a** can be detected in fresh photolysate by HPLC. **6a** was isolated as a minor product (ca. 2% theoretical yield). Nessler,[30] selective electrode, and ethylurethane GLC analyses established that ammonia is a major primary product, and outgassing the photolysate continuously into barium hydroxide showed that the same applies to carbon dioxide. These methods, together with quantitation of acetamide by GLC and of **4a** and **5a** by HPLC, afford the yield profiles shown in Figure 2. The yield of acetamide by HPLC, however, remains at 2–3% up to 60% conversion and

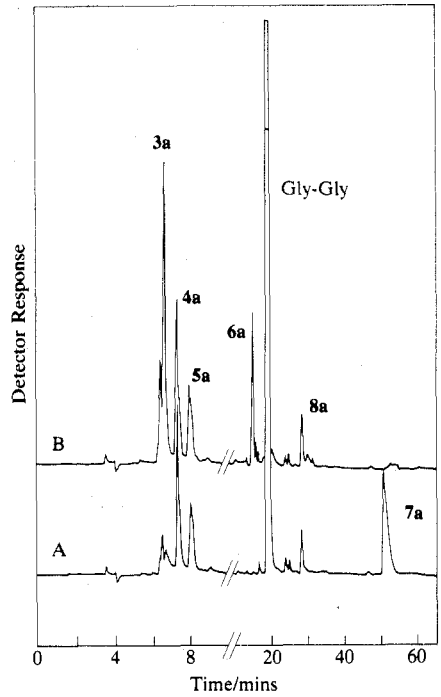

Figure 3. HPL chromatograms of aqueous glycylglycine photolysate (34% conversion) (A) before and (B) after heating at 100 °C for 20 min. SP: 2 × S5 ODS2 (250 × 5 mm). MP: 2.5×10^{-4} sodium octanesulfonate in 5×10^{-4} KH_2PO_4, pH 2.6. λ, 215 nm; FR 1 mL/min.

climbs to only 9% at 93% conversion. Although GCFTIR analysis shows that **4a** does degrade to acetamide under the GLC conditions (215 °C), thermal behavior at lower temperatures reveals that it is not the main precursor of the substantially larger quantity of acetamide found by GLC. Thus, when a photolysate at 34% conversion is held at 100 °C for 20 min, the acetamide peak in the chromatogram increases by a factor of 14, while that for **4a** remains unchanged. Moreover, this is accompanied by the loss of a significant peak with a comparatively long retention time (Figures 3 and 4). The labile compound, isolated by preparative HPLC, degrades at 100 °C to glycylglycine and acetamide in 0.8:1.0 molar ratio. The thermolysis mixture also contains 0.13 molar equivalent of formaldehyde, analyzed as its 2,4-dinitrophenylhydrazone. The original compound degraded slowly in the HPLC eluent (0.02% trifluoroacetic acid) at room temperature. The 90-MHz ^1H and ^{13}C NMR spectra in D_2O of a lyophilized sample showed signals consistent with an approximately equimolar mixture of acetamide and the TFA salts of glycylglycine and **7a** (^1H δ 2.00, 3.88, 3.94; ^{13}C δ 23.6, 43.5, 47.1, 53.5). After the

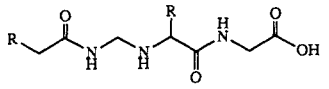

7

sample was heated for 30 min at 80 °C, the signals at 2.00 and 3.88 ppm had disappeared and the ^{1}H spectrum closely resembled that of a mixture of acetamide and glycylglycine.

Heating the photolysate also introduces a further peak in the HPL chromatogram (at 16 min in Figure 3B) whose rate of growth differs significantly from that of acetamide (Figure 4) and which was shown to be due to **6a**. Formaldehyde, which can be isolated from and detected by HPLC in fresh photolysate as its 2,4-dinitrophenylhydrazone, increases in concentration initially on heating, but then decreases. The data in Figures 3 and 4 are consistent with the rapid thermal degradation of **7a** and slow condensation of the formaldehyde released with acetamide and, possibly, other components of the photolysate, including glycylglycine. The slight increase in acetamide on extended heating (Figure 4) is accommodated by slow thermal decomposition of **4a** (Scheme I).

Glycine, glycine methylamide (**8a**), and methylamine were identified in the photolysate as trace products (<5%), and at >90% conversion, traces of glyoxylic acid could be detected and a small amount of *N*-methyloxamide isolated by liquid–liquid extraction. Yields of the major products at 20% conversion are given in Table I.

The quantum yield for decomposition of glycylglycine was determined by using a low-pressure mercury arc and hexan-2-one and 1,3-dimethyluracil as actinometers. The data in Figure 5 are based on excitation by 254-nm radiation which comprised more than 90% of the energy emitted but which was not completely absorbed by the sample (~27%). Although the lamp employed may emit some of the remaining energy at 185 nm, which would have been completely absorbed, the lack of special precautions to eliminate oxygen and cooling water impurities from the optical path, together with the optical properties of the quartz apparatus, make it very unlikely that significant photochemistry was initiated at the shorter wavelength.

Photolysis at pH 1 proceeds cleanly at a comparable rate to that at pH 6 but gives a different product distribution (Figure 6; Table I). While carbon dioxide remains a major product, ammonia, acetamide, and *N*-(hydroxymethyl)acetamide are minor products, the major involatiles being glycine methylamide (**8a**) and *N*,*N*′-diglycylethane-1,2-diamine (**9a**). **9a** was characterized spectroscopically and by comparison with a sample synthesized from CBZ-glycine *p*-nitrophenyl ester and ethane-1,2-diamine. The yields from this photolysis given in Table I are sustained between 20% and 70% conversion.

Photolysis at pH 12 yields comparable amounts of **8a** to that at pH 1, whereas this product is barely detectable at pH 6. No trace of **9a** was detected at pH 12. **8a** was also found to be a

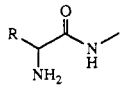

8

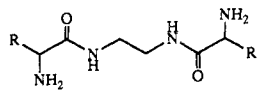

9

principal product of photolysis of a film of crystalline glycylglycine. The 28% yield observed probably understates its significance, considering the inhomogeneity of the photolyzed sample. **5a** (8%) was the only other product identified.

***N*-Acetylglycine.** Simultaneous photolysis of 0.03 M aqueous *N*-acetylglycine at pH 2.7 and pH 7.7 results in 32% and 13% conversion, respectively, after 24 h. *N*-Methylacetamide and *N*,*N*′-diacetylethane-1,2-diamine are formed in both cases in equivalent yields at pH 2.7 (19%) and in 29% and 6% yields, respectively, at pH 7.7.

DL-Alanylglycine. The photolytic behavior of DL-alanylglycine is closely analogous to that of glycylglycine. Products are formed

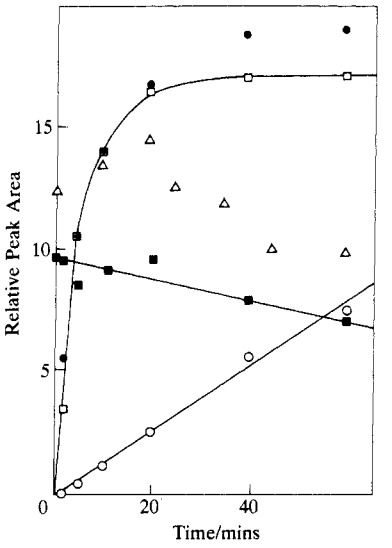

Figure 4. Change in HPLC peak areas on heating aqueous glycylglycine photolysate (34% conversion) at 100 °C. (□) Units lost from 52-min peak; (●) 3 times area gained by peak due to **3a**; (■) 3 times area of peak due to **4a**; (○) 0.3 times area gained by peak due to **6a**; (△) 0.3 times area of peak due to formaldehyde DNP (separate analysis).

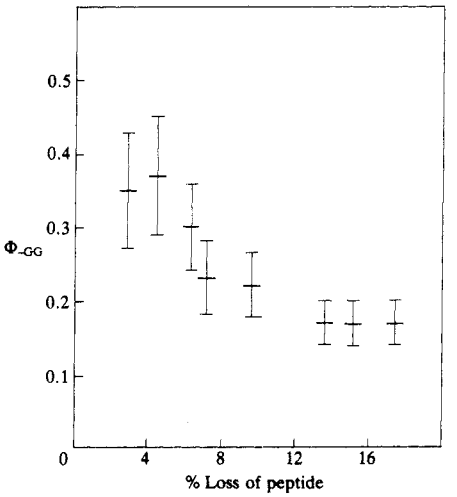

Figure 5. Quantum yield for the loss of glycylglycine by photolysis at 254 nm.

Scheme I

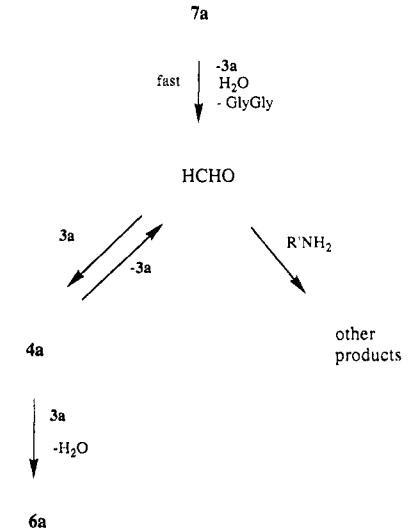

in similar yields (Table I) and include a thermally labile one whose decomposition coincides with the production of propanamide. The

Table I. Product Distributions (Percent) in the Photolyses of Dipeptides[a]

peptide	phot cond[b]	NH_3	CO_2	3[c]	4	8	9	R
Gly-Gly	5.7	65	53	55	34	<5	<1[d]	H
	1.0	12	76	<5	2	31	55	
	12.0	–[e]	–	–	15	20	<1	
	cryst	–	–	<10[f]	<1	28	<1	
Ala-Gly[g]	5.7	70	50	50	11	<5	–	CH_3
	1.0[h]	15	70	–	7	40	40[i]	
Val-Gly	5.6	45	68	45	10	<5[j]	<1	$(CH_3)_2CH$
Pro-Gly	5.4	–	23	11[k]	24[l]	–	–	$H_2N(CH_2)_3$[m]
	1.0	–	100	–	<1	10	60	
Phe-Gly	5.6	28	30	25	6	<5	–	$PhCH_2$
	1.0	7	25	–	<2	<5[n]	<1	
Gly-Phe	5.7	50	10	35[p]	–	–[q]	–	H
Pro-Phe	6.3	–	10	6[k]	–	–	–	
Phe-Pro	5.4	30	30	–	–	–	–	

[a] At 20% conversion unless indicated otherwise. [b] Initial pH. [c] By GLC. [d] Below detection limit. [e] Not measured. [f] By HPLC after 100 °C for 30 min. [g] Racemic mixture. [h] 90% conversion. [i] 1:1 mixture of diastereoisomers. [j] 22% by GLC. [k] As 2-piperidone. [l] **13b**. Assumes ϵ_{215}(**13b**)/ϵ_{215}PG = ϵ_{215}(**4a**)/ϵ_{215}GG. [m] Proline ring unbroken in **8** and **9**. [n] Increases on heating; 10% isolated. [p] By HPLC on fresh photolysate. [q] The corresponding compound, glycine (2-phenylethyl)amide, is present in trace amounts.

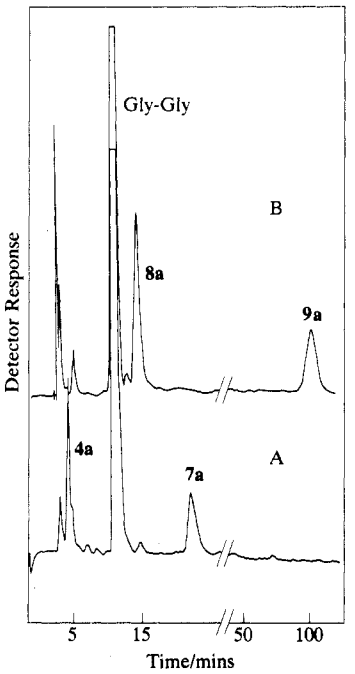

Figure 6. HPL chromatogram of aqueous glycylglycine photolysates (30% conversion) (A) with initial pH 5.7 and (B) with initial pH 1.0. Conditions as for Figure 3 except that a single column was used.

yield profile for **4b** differs from that of the other products, as seen with glycylglycine (Figure 2), and analogous minor products **5b** and **6b** were isolated together with **10b**. [**10a** was not isolated

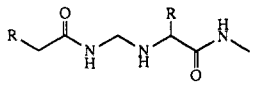

10

from the photolysate of glycylglycine but was observed as a minor component of the dichloromethane extract (^{1}H NMR (DMSO-d_6) δ 1.84 (s, 4 H), 2.65 (d, 3H), 2.81 (s, 2H), 3.60 (d, 2H), 7.72 (b, 1H), 8.08 (b, 1H))]. Photolysis at pH 1 gives **8b** and a product appearing as a highly retained pair of peaks in HPLC, fully consistent with the diastereomers of **9b** expected from the racemic substrate.

Valylglycine. A lower yield of ammonia is obtained in the photolysis of valylglycine than in those of the first two dipeptides, and **6c** was not detected among the minor products. In other respects, however, the photochemistry of this dipeptide follows the previous pattern. Thus, the yield of **3c** increases from less than 5% to more than 40% when the photolysate is heated at 100 °C for 30 min, while that of **4c** remains unchanged. The yield of **4c** falls much more rapidly than those of the other products as the photolysis proceeds. **5c** is a minor component of the

Scheme II

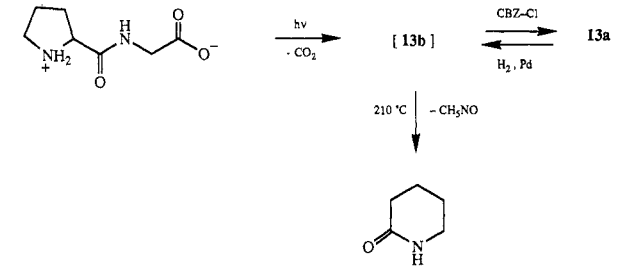

photolysate (<1% yield). Significantly more than **10** (**10c**) was recovered from a dichloromethane extract of the photolysate in this case (ca. 5% based on 2 mol of substrate). Thermolysis in GCFTIR analysis shows **10c** degrades readily to **3c**, **8c**, and two

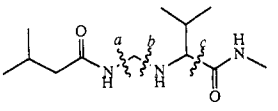

10c

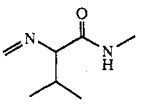

11

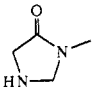

12

products whose gas-phase spectra are consistent with **11** (ν_{max} 3345, 3021, 2969, 2882, 1709, 1665, 1510 cm^{-1} and **12** (ν_{max} 3364, 1729 cm^{-1}). This reaction accounts for the much higher yield of **8c** reported by GLC than by HPLC. Moreover, the CI mass spectrum of **10c** shows analogous fragmentations **a** and **b** in addition to **c**.

Prolylglycine. Prolylglycine is distinctive in the present context as deamination would be expressed as ring opening rather than as loss of ammonia. Photolysis at pH 6 is again accompanied by increasing pH, although to a greater extent than with previous peptides (Figure 1). Tests with Nessler's reagent show that this is not due to release of ammonia. An amine fraction of the photolysate was obtained by cation-exchange chromatography and derivatized with benzyl chloroformate. Separation by preparative normal-phase HPLC gave the bis-CBZ derivative, **13a**, of 5-amino-*N*-(hydroxymethyl)pentanamide (**13b**). Hydrogenolysis of **13a** affords a solution of a compound shown by HPLC under five separate conditions to be an important component of the original photolysate. When analyzed by GCFTIR, both this solution and the photolysate give a component with the gas-phase spectrum of 2-piperidone, a product that might be expected from a thermally induced cyclodeamination of **13a** (Scheme II). The yields of carbon dioxide and 2-piperidone change little throughout photolysis, whereas that of **13b** falls to 12% and 6% at 30% and

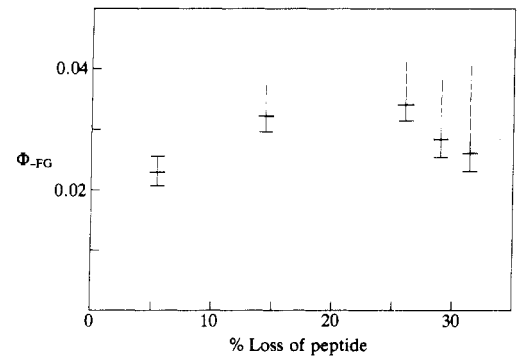

Figure 7. Quantum yield for the photolytic loss of phenylalanylglycine.

70% conversion, respectively (cf. Table I), thus following the trends (Figure 2) seen in previous photolyses.

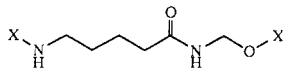

13 a X = $PhCH_2OCO$ b X = H

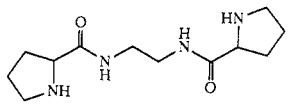

9e

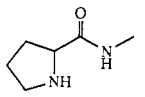

8e

Photolysis at pH 1 follows the same pathway as that of glycylglycine. Highly efficient decarboxylation accompanies the formation of *N,N'*-diprolylethane-1,2-diamine (**9e**) and, in lower yield, proline methylamide (**8e**).

Phenylalanylglycine. Photolysis of phenylalanylglycine gives many more products than are seen with aliphatic dipeptides. Moreover, some complex high molecular weight material is deposited during the irradiation, accounting for almost 10% of photolyzed peptide. Nevertheless, a rise in pH was again observed, and the products identified include compounds analogous to those found with aliphatic dipeptides (Table I). Thus, maintaining the photolysate at 100 °C for 30 min causes the area of the peak for **3d** in HPLC to increase 4-fold concomitantly with the loss of a highly retained peak. **4d** remains unaffected by these conditions and, following the usual behavior, its yield falls rapidly in the early stages of photolysis. Yields generally are significantly lower than those of the corresponding products in the aliphatic series (Table I). Traces of **5d** were detected, but this compound is more photochemically labile than the substrate. Of other products reported previously,[17] we found glycine, 3-benzylpiperazine-2,5-dione (10% and 1%, respectively at 25% conversion), and traces of phenylalanine and glycylglycine. Additionally, ca. 1% toluene was established by GC analysis.

The initial quantum yield for the loss of phenylalanylglycine is about 0.02 (Figure 7). Competitive absorption by products probably means that values at higher conversions are greater than those observed and that the quantum yield increases initially as photolysis proceeds.

As with glycylglycine, less ammonia is released in photolysis at low pH. The yield of **8d** by analysis of the photolysate was much lower than that isolated after liquid–liquid extraction. The amount of **8d** in the photolysate increases on heating, however, typically, 4-fold after 1 h at 100 °C. Photolysis of **8d** at pH 1 yields 15% ammonia at 20% conversion.

Scheme III

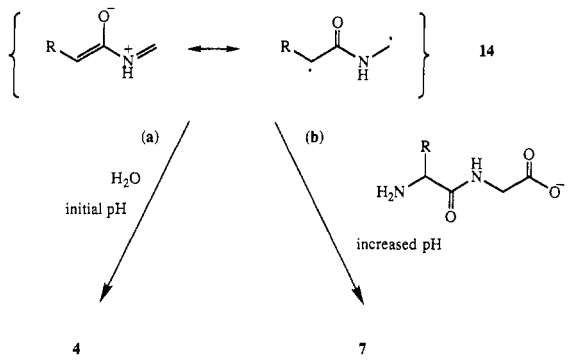

Glycylphenylalanine. An aqueous solution of glycylphenylalanine becomes pink on irradiation, and a precipitate of complex constitution is deposited (ca. 15% of the mass of reacted dipeptide at 40% conversion). The photolysate contains a large number of other products, including a significant amount of acetamide, contrasting with glycylglycine photolysis where this product appears in quantity only after heating. Ammonia is enhanced and carbon dioxide reduced compared with yields from the retropeptide. 3-Benzylpiperazine-2,5-dione[17] was found in 6% yield at 20% conversion.

Prolylphenylalanine and Phenylalanylproline. These dipeptides are by far the most labile of those examined. Typically, 35% loss occurs after 15 min of irradiation by method B, while under comparable conditions less than 5% of phenylalanylglycine has reacted. The photolysates become pink, their pH values increase and, in the case of phenylalanylproline, a deposit of complex constitution is thrown down. The pink color develops in the dark after a short period of irradiation and fades on exposure to air. Prolylphenylalanine releases carbon dioxide to a small extent, and GCFTIR analysis of the photolysate reveals a comparable yield of 2-piperidone. The yields of ammonia and carbon dioxide from phenylalanylproline are similar to those from phenylalanylglycine. We were unable to isolate other photoproducts from either dipeptide.

Discussion

At 5% reaction, the principal products in the photolysis of neutral aqueous glycylglycine are ammonia (75%), carbon dioxide (65%) and *N*-(hydroxymethyl)acetamide (65%). Although evidence for some deamination and decarboxylation[5,16,17] has been noted, this result contrasts with reports that neither decarboxylation or deamination radicals are important transients in neutral photolysates.[20,25] Moreover, we have shown that the only products other than ammonia that have been identified previously, glycine methylamide, methylamine, and glycine,[17] are present in only trace amounts (2%, 1%, and <1%, respectively, at 20% conversion).

We suggest our results are best explained by assuming the outcome of deamination and decarboxylation is the formation of the resonance-stabilized intermediate **14a**. The ground state of **14a** is zwitterionic rather than diradical,[55] so no unpaired spin would be observed, and further reaction would be by nucleophilic addition rather than hydrogen abstraction or cyclization. We failed to detect *N*-methylacetamide, 2-azetidinone, or β-alanine in the photolysate. Initially, the strongest nucleophiles available are water and the peptide carboxylate group which, considering both nucleophilicity and concentration, might be expected to be comparably effective. In the event, attack by water dominates and, as with the closely similar acyliminium compounds,[56] the *N*-(hydroxymethyl)amide is formed (Scheme IIIa). As the photolysis proceeds, however, the rapid increase in pH following deamination makes available increasing amounts of the more nucleophilic conjugate base of the peptide (typically, 40-fold after 45% conversion) and the thermal precursor of acetamide, **7a**,

(55) Aoyama, H.; Sakamoto, M.; Kuwabara, K.; Yoshida, K.; Omote, Y. *J. Am. Chem. Soc.* **1983**, *105*, 1958–1964.
(56) Speckamp, W. N.; Hiemestra, H. *Tetrahedron* **1985**, *41*, 4367–4416.

Scheme IV

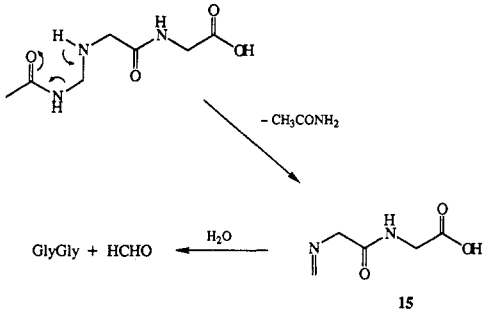

becomes the more significant adduct (Scheme IIIb). Peptide–NH rather than peptide–OH addition in **7a** is supported by the ^{13}C chemical shift of the new methylene carbon atom at 53.5 ppm in D_2O [cf. 63 ppm for *N*-(hydroxymethyl)acetamide]. The yield of **7a**, expressed as its HPLC peak area divided by the fraction of substrate consumed, increases with conversion, complementing the behavior of the yield of the competing adduct with water (Figure 2). In GLC analysis, both **5a** and **7a** degrade to acetamide, thus accounting for the high and relatively constant yield of the latter obtained this way.

The formation of glycylglycine, acetamide, and formaldehyde from **7a** at 100 °C may occur via a six-membered transition state and the imine **15** (Scheme IV). The extra step required to release glycylglycine would then account for its small deficit relative to acetamide. Moreover, indirect support for the transitory existence of an imine was frequently observed as a signal near 8 ppm in the ^1H NMR spectra of photolysate samples in D_2O. The thermolysis is similar to the thermal decomposition of bisamidomethanes[56] but occurs more readily as bisacetamidomethane (**6a**), formed when the photolysate is heated, survives these conditions. The absence of **6a** from fresh photolysate indicates it is not formed directly from **14a**.

Our results suggest the oxidative pathway for peptide photodegradation,[16,57] leading ultimately in this case to glyoxylic acid, is unimportant. The trace amounts of glyoxylic acid detected and the small amount of *N*-methyloxamide recovered at high conversion probably arise via the formation of the stabilized α-carbon radicals[58] adjacent to carboxyl and amino groups, respectively, and complement the presence of the reduction product, *N*-acetylglycine.

The trapping of some glycylglycine in a thermal reaction following photolysis means that product yields based on photolyzed peptide are higher than those observed (which are based on peptide consumed) by a factor $f = P/(P - A + H)$, where P is the observed molar loss of peptide, A is the molar yield of acetamide by GC, and H is the molar yield of *N*-(hydroxymethyl)acetamide by HPLC. The low yield of acetamide measured by HPLC affects f differently according to whether it arises via **14a** or via some other route, such as photolysis of *N*-(hydroxymethyl)acetamide[59] but only to a very small extent (±2%). f is 1.25 at 20% conversion, giving photolysis yields of 81%, 66%, 69%, and 42% for ammonia, carbon dioxide, acetamide by GC, and *N*-(hydroxymethyl)acetamide by HPLC, respectively. This high mass balance infers a uniquely favorable pathway for the photodegradation of aqueous glycylglycine.

Quantum yield measurements were also based on observed loss of peptide. They were conducted with solutions 70 times more concentrated than those used in other photolyses. Although the same range of products was observed, the competition between water and the conjugate base of glycylglycine for trapping **14a** would favor the peptide in the concentrated solution. The involvement of glycylglycine in trapping **14a** means two molecules of the substrate are lost for each photon absorbed, and the quantum yields for photolytic loss of dipeptide above 10% conversion are half those shown in Figure 4 (i.e., $f = 2$). Product analyses below 10% conversion were not sufficiently accurate to allow us to estimate from the data the concentration effect on the initial quantum yield, but the calculated concentration of the conjugate base at the initial pH is 6.5×10^{-3} M, which, corresponding to 45% conversion with an initial substrate concentration of 0.03 M, suggests an f value of 1.43. Hence, the initial quantum yield for photolytic loss of glycylglycine is estimated to be 0.3 ± 0.1.

Scheme V

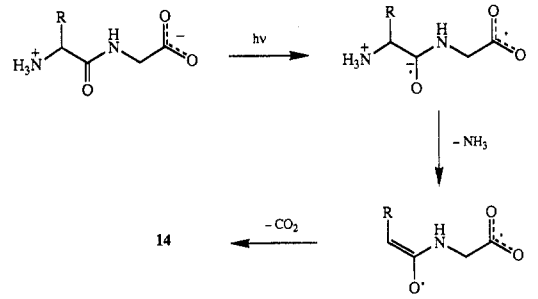

The high quantum yield for the photodegradation of glycylglycine accords with the noted photolability of peptides.[4-6] One might expect absorption above 220 nm to be due principally to the n → π* transition of the amide group. Absorption by glycylglycine in this region, however, shows an interesting dependence on pH, having lower molar absorbtivity when the carboxyl group is protonated,[60] while the reverse is true for acetic acid.[61] Asher has suggested this may be understood in terms of electrostatic effects on the 190-nm amide π → π* transition.[62] An alternative hypothesis is that additional absorption in zwitterionic glycylglycine is a consequence of orbital coupling between carboxylate and amide groups, where electronic excitation results in a charge-transfer transition. Considered as photoinduced electron transfer, the corresponding "back-reaction" is internal conversion to S_0. Inhibition by, for example, intersystem crossing,[63] would then allow ejection of ammonia and loss of carbon dioxide to give **14a** (Scheme V). The same outcome, however, could follow an unperturbed amide n → π* transition, as the excited acceptor, CONH*, has ready access to both a good donor, $-CO_2^-$, and a molecular fragmentation that competes effectively with the back-reaction.[64] Photoinduced decarboxylation is a well-known electron-transfer process,[65] and ab initio SCF studies of glycylglycine predict a surprisingly low (carboxylate) ionization potential.[66] Photoinduced one-electron reductions of peptide carbonyl are also widely reported,[1-3] although the latter are usually promoted by donor excitation. Electron transfer in the present case would have a transition state closely similar to that for the highly favorable charge-transfer quenching in 2-(2,2-diaminoethyl)acetophenone[67] and one that accommodates the requirement in n → π* excitation of an in-plane approach by the donor.[68] The primary fragmentation is more likely to be deamination than decarboxylation, as the need for some conformational change between electron transfer and decarboxylation is anticipated,[67]

(57) Meybeck, A.; Meybeck, J. *Photochem. Photobiol.* **1967**, *6*, 365–378.
(58) Easton, C. J.; Hay, M. P. *J. Chem. Soc., Chem. Commun.* **1986**, 55–57.
(59) This reaction was observed but is much less efficient than the photolysis of glycylglycine.
(60) Saidel, L. J. *Arch. Biochem. Biophys.* **1955**, *56*, 45–58.
(61) Claesson, I. M. *Ark. Kemi* **1956**, *10*, 1–102.
(62) Song, S.; Asher, S. A. *J. Am. Chem. Soc.* **1989**, *111*, 4295–4306.
(63) Mauzerall, D. C. In *Photoinduced Electron Transfer*; Fox, M. A., Chanon, M., Eds.; Elsevier: Amsterdam, 1988; pp 228–244.
(64) (a) Eaton, D. F. *Pure Appl. Chem.* **1984**, *56*, 1191–1202. (b) Fox, M. A. *Adv. Photochem.* **1986**, *13*, 237–327.
(65) (a) Baezold, D.; Fassler, D. *Z. Chem.* **1985**, *25*, 154–156. (b) Carmichael, A. J.; Mossaba, M. M.; Reisz, P.; Rosenthal, I. *Photobiochem. Photobiophys.* **1985**, *10*, 13–21. (c) Davidson, R. S.; Goodwin, D. *J. Chem. Soc., Perkin Trans. 2* **1982**, 1559–1564. (d) Kuruchi, Y.; Ohga, K.; Nobuhara, H.; Morita, S. *Bull. Chem. Soc. Jpn.* **1985**, *58*, 2711–2712. (e) Das, S.; Johnson, G. R. A.; Nazhat, N. B.; Sandalla-Nahzat, R. *J. Chem. Soc., Faraday Trans. 1* **1984**, *80*, 2759–2766.
(66) Wright, L. R.; Borkman, R. F. *J. Phys. Chem.* **1982**, *86*, 3956–3962.
(67) Wagner, P. J. *Acc. Chem. Res.* **1983**, *16*, 461–467.
(68) Kavarnos, G.; Turro, N. J. *Chem. Rev.* **1986**, *86*, 401–449.

Table II. Conformational Parameters for Glycylglycine

	min intramol O–O distance, nm	C_α (NH_3^+), deg ψ_1[a]	$C_\alpha(CO_2^-)$, deg	
			ϕ_2	ψ_2
cryst (α form)[b]	0.48	152	155	170
optimal for Scheme V or cyclodeamination	<0.25	±90	−30 to 30	−30 to 30
		±90	−30 to 30	150 to −150
optimal for continuous transformation	~0.38	−90	−90	0
		90	90	0
calcd for aq soln	~0.25[c]	−155	−76	165[d]
	<0.25[c]		−73	−145[e]

[a] ϕ_1 irrelevant. [b] Reference 71. [c] Estimated, using $\phi_2\psi_2$. [d] Reference 72. [e] Reference 73.

Scheme VI

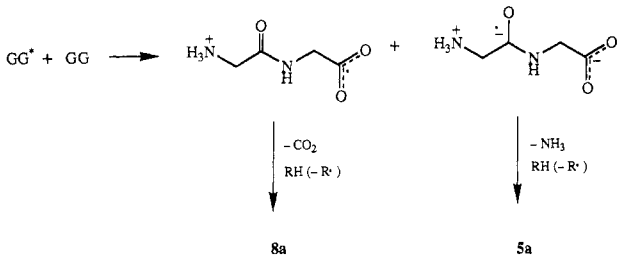

8a **5a**

whereas this is not necessarily so for deamination. Deamination following (external) electron addition to carbonyl is a primary reaction in the radiolysis of peptides.[3] With glycylglycine this would leave a carboxylate ion. In photoinduced intramolecular electron transfer, however, deamination leaves a carboxy radical which is more readily disposed to further fragmentation.

Plausible alternatives to Scheme V include O–O cyclodeamination (promoted by reversed polarity in the n → π* state) followed by ring-opening decarboxylation and concerted deamination and decarboxylation in a continuous transformation of the excited state.[69]

Whichever hypothesis is correct, access to suitable conformations is an important constraint[67] and applies particularly when the results of photolysis in solution are compared with those in the crystalline state.[70] Relevant torsional parameters and carboxylate–amide O–O distances for glycylglycine are given in Table II and show that none of the mechanisms considered for its photochemistry in solution is likely to operate in the solid state. The comparatively high yield of glycine methylamide (**8a**) we observed in solid-state photolysis, together with the absence of adducts of **14a**, is consistent with this prediction. Our results would be explained by electron transfer between molecules, noting their head-to-tail arrangement in the lattice with an intermolecular O–O distance of 0.34 nm[71] (Scheme VI). We found both decarboxylation and deamination products, where the comparatively low yield of the latter might be expected from its own photolability (ref 18 and see later). ESR studies of dipeptide photolyses in the solid state support the initial formation of decarboxylation radicals[22] and the suggestion that the release of carbon dioxide is followed by hydrogen abstraction.[18] Authors of the latter, however, detected no ammonia in the solid-state photolysis of glycylglycine.

Table II also includes conformational parameters calculated to be most favorable for glycylglycine in aqueous solution, and while some values differ significantly from those optimal for the mechanisms considered, they are less restrictive than in the solid state. The values for the "continuous transformation" pathway also coincide with those estimated to give the best solvation for glycyl within proteins and are frequently observed in spite of unfavorable van der Waal interactions.[74]

Scheme VII

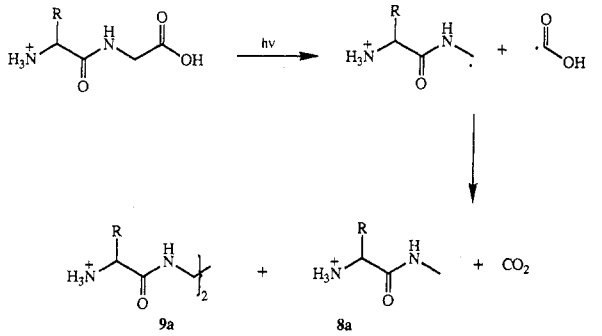

9a **8a**

Scheme VIII

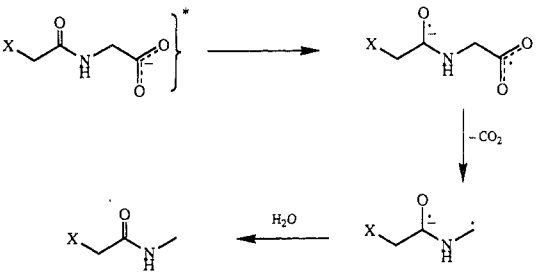

a, X = NH_2; b, X = $\overset{+}{N}H_3$; c, X = H

Protonation of the carboxyl group profoundly affects the course of photodegradation of small peptides in aqueous solution. Both flash photolysis[20] and ESR spin-trapping[25] studies suggest homolysis of the C_α–CO_2H bond occurs readily but that this ceases to be important when the carboxyl group is deprotonated. The present results support this suggestion (Scheme VII). Both the predicted radical dimer[20] and the methylamide are formed in good yield, while compounds typical of photolysis at (initial) pH 6, including ammonia, are minor products. Protonation of the carboxyl group would be inhibitory in both charge-transfer and n → π* electron-transfer models for the photochemistry of dipeptides at pH 6. At low pH, radiation above 200 nm is absorbed significantly by transitions localized in the carboxyl group, prompting α-cleavage chemistry typical of simple carboxylic acids.[75]

Glycine methylamide, but not the radical dimer, **9a**, is a significant product of photolysis when the initial pH is 12. With deamination unfavorable, photoinduced electron transfer is followed only by decarboxylation and protonation (Scheme VIIIa). A similar mechanism might also explain the origin of the small amount of this product found under neutral conditions if electron transfer occurs in a conformation that inhibits deamination (Scheme VIIIb). It may also apply in the aqueous photochemistry of ionized *N*-acetylglycine. Hayon reported the formation of decarboxylation radicals in the photolysis of the protonated compound in aqueous solution,[20] and we have found that under

(69) Morrison, H.; Muthuramu, K.; Pandey, G.; Severance, D.; Bigot, M. *J. Org. Chem.* **1986**, *51*, 3358–3363.
(70) Zimmerman, H. E.; Zuraw, M. J. *J. Am. Chem. Soc.* **1989**, *111*, 2358–2361.
(71) Biswas, A. B.; Hughes, E. Q.; Sharma, B. D.; Norton Wilson, J. *Acta Crystallogr.* **1968**, *B24*, 40–50.
(72) Destrade, C.; Garrigou-Lagrange, C. *J. Mol. Struct.* **1976**, *31*, 301–317.
(73) David, F.; David, P. G. *J. Phys. Chem.* **1976**, *80*, 579–583.
(74) Ponnuswamy, P. K.; Manavalan, P. *J. Theor. Biol.* **1976**, *60*, 481–486.
(75) Givens, R. S.; Levi, N. In *The Chemistry of Carboxylic Acids and Esters*; Patai, S., Ed.; Wiley: New York, 1979; Suppl. B, Part 1, p 671.

Scheme IX

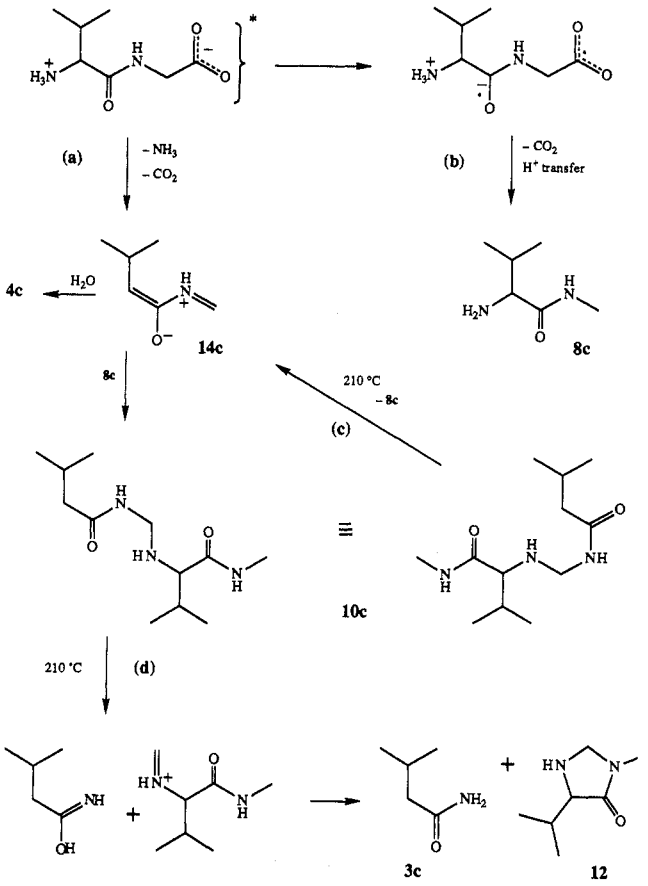

similar conditions both the dimer, *N*,*N*′-diacetylethane-1,2-diamine, and the product from hydrogen abstraction, *N*-methylacetamide, are significant products with equal yields (19%). Hayon noted, however, that the yield of radicals decreases markedly above pH 3, yet carbon dioxide remains an important product.[76] Moreover, we have found that although the yield of *N*-methylacetamide remains significant in photolysis at pH 7.7 (26%), that of the radical dimer is then only 6%. Decarboxylation and the formation of *N*-methylacetamide without the involvement of the monoradical are fully accommodated by the electron-transfer mechanism depicted in Scheme VIIIc.

Substitution at the amino α-carbon with methyl or 2-propyl has little effect on the photochemistry demonstrated by glycylglycine (which also accounts satisfactorily for most of the results already reported for these dipeptides[4,16,25,26]). In particular, we found no evidence in the photolyses of alanylglycine and valylglycine for the formation of unsaturated amides, or their photoproducts, that might be expected to follow a facile 1,5-hydrogen shift in the diradical form of **14b** or **14c**.

The observed yields of ammonia and hydroxymethylamide are lower for valylglycine, while that of carbon dioxide is enhanced. It seems probable that the bulky *N*-Cα substituent makes the conformation required for deamination less readily available than in glycylglycine (Scheme IXa), allowing decarboxylation and proton transfer to be more competitive (Scheme IXb). Moreover, the resulting valine methylamide, **8c**, competes effectively with water for the intermediate **14c** arising from deamination, and a significant yield of the adduct **10c** results at the expense of the hydroxymethylamide, **4c**. In contrast with the photolysis of glycylglycine, **8c** accompanies **4c** as one of the first observable products in the photolysis of valylglycine but is consumed by adduct formation subsequently. The latter was observed in the photolysates of alanylglycine and glycylglycine, but to a lesser extent. The formation of **10c** is reversed at 210 °C (Scheme IXc),

(76) Hill, D. J. T.; O'Donnell, J. H.; Pomery, P. J.; Whittaker, A. K. *Polym. Photochem.* **1986**, *7*, 13–25.

Scheme X

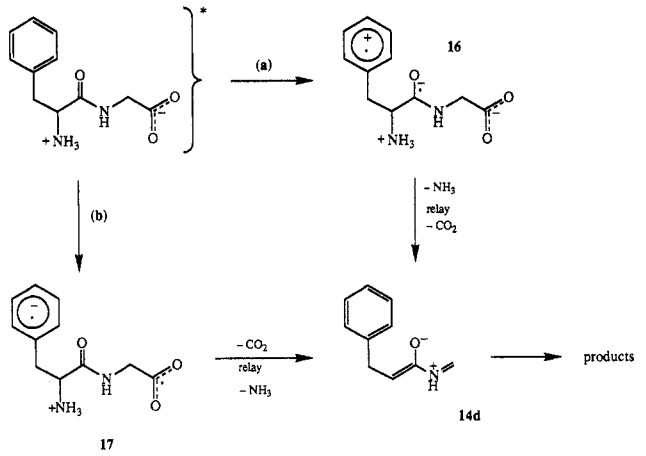

releasing valine methylamide that accounts for more than 20% of photolyzed peptide. The accompanying alternative fragmentation shown in Scheme IXd accounts for the other thermolysis products observed.

The photolytic ring opening of prolylglycine at pH 5.4 predicted by the general mechanism is observed, but the products monitored account for only 25% of degraded peptide. The comparatively large increase in pH (Figure 1) reflects the formation of a primary amine rather than ammonia, so the degradation pathway probably branches after the ring-opening step. The latter is consistent with reports of an analogous process following external electron addition in the radiolysis of prolyl peptides.[77] Quantitative decarboxylation and the formation of the radical dimer in photolysis at pH 1 follow the pattern observed with glycylglycine and emphasize the sensitivity of the photochemistry to protonation of the carboxyl group.

Zwitterionic phenylalanylglycine also undergoes, to a lesser extent, the photochemistry shown by glycylglycine. As with valylglycine, some conformational inhibition of deamination might be expected, but the depressed yield of carbon dioxide suggests competition from alternative pathways is also involved. We confirm Meybeck's qualitative observations of 3-phenylpropanamide (**3d**), phenylalanine methylamide (**8d**), glycine, glycylglycine, phenylalanine, and 3-benzylpiperazine-2,5-dione,[17] but all except the first, which is the analogue of acetamide in the photolysis of glycylglycine, and glycine are minor products. We did not detect the deamination product which might be expected from the corresponding radical observed by ESR,[78] although benzyl radicals, which are also reported,[21,24,78] accord with our finding toluene in trace amounts.

Phenylalanylglycine differs from the other dipeptides studied in that the most active chromophore lies in the side chain. The electronic absorption spectrum of the peptide in water is effectively the sum of the spectra of benzyl alcohol and glycylglycine, so the absorption of 254-nm radiation may be considered to result in excitation affecting predominantly the phenyl ring. The initial quantum yield for the formation of **3d** is 5.6 ($\pm$1.7) $\times$ 10^{-3}. As intramolecular energy transfer from phenyl to peptide groups is precluded,[79] the formation of **3d** via peptide excitation could occur only by direct absorption. Competitive absorption by phenyl,[5] and the conditions of measurement, however, reduced the theoretical quantum yield of unity by this mechanism to a maximum observable value of 4.5 $\times$ 10^{-3}. Thus, either the formation of **3d** via the photolytic pathway for aliphatic peptides has an effective quantum yield near unity or the observed data reflect the efficiency with which a similar chemistry arises via absorption in the side chain.

(77) (a) Makino, K.; Riesz, P. *Can. J. Chem.* **1982**, *60*, 1480–1485. (b) Suzuki, W.; Matino, K.; Moriya, F.; Rokyshika, S.; Hatano, H. *J. Phys. Chem.* **1981**, *85*, 263–268.

(78) Lion, Y.; Kuwabara, M.; Riesz, P. *Photochem. Photobiol.* **1981**, *34*, 297–307.

(79) Larson, D. B.; Arnett, J. F.; Seliskar, C. J.; McGlynn, S. P. *J. Am. Chem. Soc.* **1974**, *96*, 3370–3380.

Scheme XI

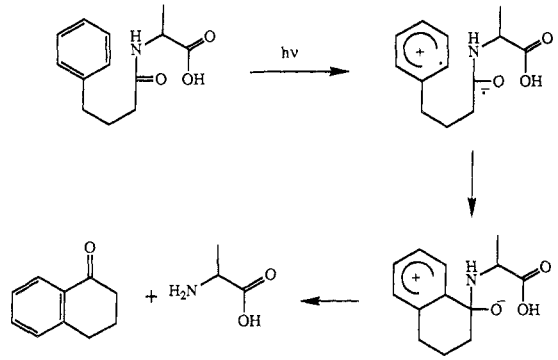

Phenyl absorption presents two opportunities for photoinduced intramolecular electron transfer: to the peptide LUMO[1,27,80] or from the carboxylic HOMO[80,81] (Scheme Xa,b, respectively). Scheme Xa would be facilitated by the tendency of the side chain to fold over the peptide group[82] and follows earlier proposals for a carboxylate-to-phenyl relay in the photolysis of phenylalanyl derivatives.[21,24,27,78] On the other hand, dye-promoted photodecarboxylations of peptides[81] demonstrate the feasibility of the alternative mode (Scheme Xb), which might also better accommodate evidence of the decarboxylation radical.[24,78] Potential can be seen in both **16** and **17** for product formation that avoids deamination, decarboxylation, or both, but, with the possible exception of glycine, no such product was detected in significant yield. In particular, none of the available compounds benzyl alcohol, coumarin, dihydrocoumarin,[83] hydrocinnamic acid, *N*-(3-phenylpropanoyl)glycine, *N*-(1-oxo-3-phenyl-2-propenyl)-glycine, and *N*-methyl-3-phenyl-2-propenamide (and their photoproducts) that might be anticipated from the intermediate **16** were found in the photolysate. The release of glycine could be the result of deamination of **16**, followed by *O*-aryl cyclization and hydrolysis. A pathway similar to Scheme Xa offers a plausible reason for the exceptionally high quantum yield for the photochemical release of alanine from the phenylacylalanine, $Ph(CH_2)_nCONHCH(CH_3)CO_2H$, when $n = 3$.[5] As shown in Scheme XI, the availability of a suitable conformation for not only electron transfer but also cyclization would account for the 10-fold higher value compared with analogous compounds where $n = 2$ or 4.

Product formation via **14d** explains results from the photolysis of phenylalanylglycine that are similar to those for glycylglycine and implicates the intermediacy of an adduct between **14d** and the substrate. This finds support in the variation of Φ_{-FG} with conversion (Figure 7), which shows the initial increase expected for the introduction, as the photolysis proceeds, of a pathway involving a second molecule of dipeptide. The effect is attenuated in Figure 7 by the opposite trend, shown at higher conversion, due to competing absorption by products.

Photolysis of phenylalanylglycine at low pH shows behavior similar to that for glycylglycine, albeit with lower yields of analogous products. The 4-fold decrease for ammonia contrasts sharply with the insensitivity of deamination to pH in this range in the photolysis of phenylalanine[84] and suggests that the involvement of carboxylate is important at the higher pH in the dipeptide, in spite of phenyl excitation. The significantly lower

Scheme XII

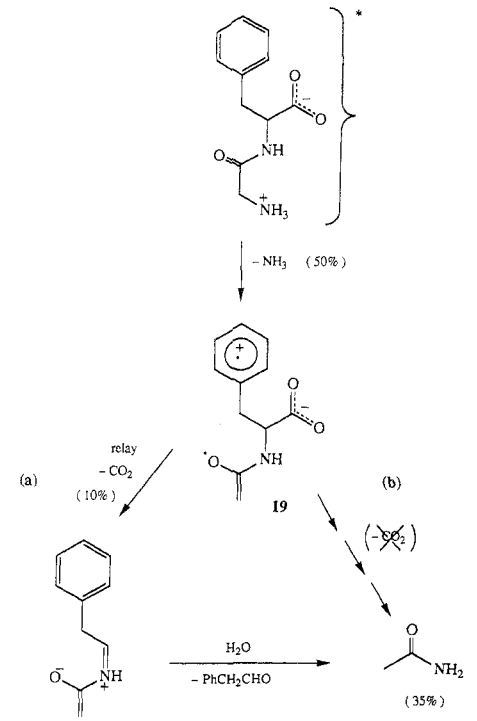

yield of ammonia from protonated phenylalanine methylamide (**8d**) compared with that from the neutral dipeptide supports the same conclusion.

The higher yield of ammonia and lower yield of carbon dioxide in photolysis of the retropeptide, glycylphenylalanine, favors electron transfer from excited phenyl to ground-state CONH (Scheme XII), as applies in analogous tryptophyl derivatives.[29] In the photolysis of glycyltryptophan, the diradical analogous to **19** undergoes cyclization and proton transfer to give **2**. We did not find a cyclized product with glycylphenylalanine but a significant yield of acetamide. The low yield of carbon dioxide, however, shows that most of this product cannot arise via electron relay and the glycylglycine mechanism (route a, Scheme XII) but must involve a pathway (b) that not only avoids the release of carbon dioxide but also accommodates the formation of acetamide directly in the photolysate. A search for some plausible products consistent with this requirement (e.g., coumarin, phenylpyruvic acid, glyoxylic acid, and benzyl alcohol) was unsuccessful, although this may have been frustrated by secondary photochemistry. Our results suggest that the only radical reported in spin-trapping studies,[78] corresponding to decarboxylation, is part of a minor degradative pathway. Meybeck detected 3-benzylpiperazine-2,5-dione, glycylglycine, glycine, and phenylalanine. We found the first of these in 6% yield at 20% conversion; the other three are, at best, very minor products of photolysis. None of the intermediates suggested in Scheme XII account readily for the piperazinedione. Analogues are not formed in the photolysis of aliphatic dipeptides, and the involvement of the excited phenyl group as an electron acceptor offers a plausible hypothesis (Scheme XIII). A conformation in which the phenyl ring lies over the peptide group[82] offers opportunities for electron transfer, proton transfer, *O*-aryl cyclization, and cyclodehydration.

Decarboxylation is also inhibited in the other C-terminal phenylalanyl peptide studied, prolylphenylalanine. The formation of 2-piperidone after heating the photolysate of this substrate indicates a ring-opening deamination occurs similar to that observed with prolylglycine (Scheme II), although the (secondary) hydroxymethylamide from prolylphenylalanine would fragment spontaneously.[56] The low yield and lack of other product data leave open the question of whether or not the reaction is promoted by side-chain absorption. The closely similar yields of carbon dioxide and ammonia for phenylalanylproline and phenylalanylglycine show that, if Scheme XI is valid, a prolyl ring applies

(80) Albini, A.; Sulpizio, A. In *Photoinduced Electron Transfer*; Fox, M. A., Chanon, M., Eds.; Elsevier: Amsterdam, 1988; Part C, p 88.
(81) Carmichael, A. J.; Mossaba, M. M.; Riesz, P.; Rosenthal, I. *Photobiochem. Photobiophys.* **1985**, *10*, 13–21.
(82) Kobayashi, J.; Nagai, V. *Biopolymers* **1978**, *17*, 2265–2277. Liwo, A.; Ciarkowski, J. *Tetrahedron Lett.* **1985**, *26*, 1873–1876. Zhang, W.; Anteunis, M. J. O.; Borremans, F. A. M. *Int. J. Pept. Protein Res.* **1986**, *28*, 593–602.
(83) (a) Pandey, G.; Krishna, A.; Rao, J. M. *Tetrahedron Lett.* **1986**, *27*, 4075–4076. (b) Fry, A. J. *Synthetic Organic Electrochemistry*; Harper and Row: New York, 1972; p 275.
(84) Mukherjee, T.; Mittal, L. J.; Mittal, J. P. *Ind. J. Chem.* **1989**, *28A*, 932–934.

Scheme XIII

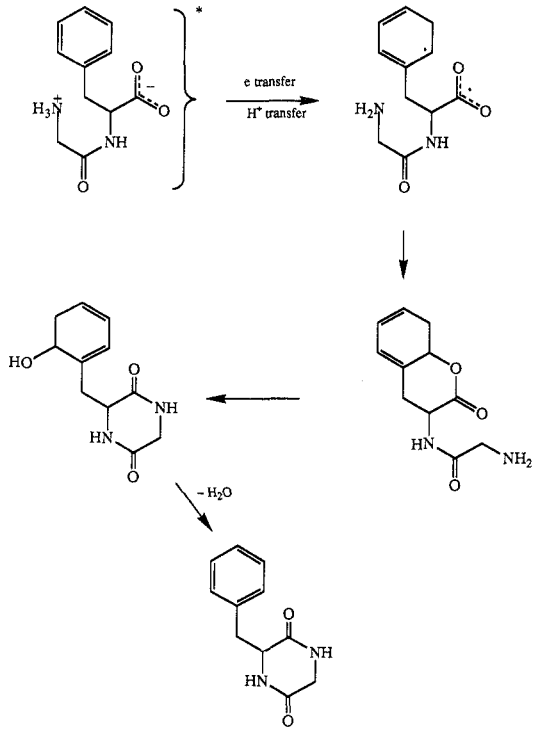

no constraint to electron transfer between the carboxylate and phenyl groups.

Conclusions

Absorption of UV radiation by the peptide group in aliphatic dipeptides leads to efficient deamination and decarboxylation. Nucleophilic addition to the zwitterionic intermediate that remains then affords the major products. Results from glycylglycine, in particular, emphasize the need for caution in evaluating data from the observation of transients. Acetamide and its thermal precursors, accounting for ~70% of the photoproducts, have hitherto remained undetected.

The primary photochemistry can be explained in terms of intramolecular electron transfer from carboxylate to n → π* excited amide or, possibly, of bond cleavage promoted by polarization in a charge-transfer excited state. Both protonation of carboxylate and deprotonation of ammonium groups lead to different photochemistry, the former because of the increased ionization potential of the incipient donor[85] and the latter because deamination is inhibited. The high-yield products at low pH arise from hydrogen abstraction by, and dimerization of, the decarboxylation radical.

Substitution at the amino α-carbon atom reduces the availability of conformations required for deamination, and products derived from decarboxylation alone are formed in higher yield. Ring-opening deamination remains a principal outcome, however, in the photolysis of neutral aqueous prolylglycine. Phenylalanyl peptides degrade via similar intermediates, implicating side chain to peptide electron transfer[19,21,28,29] as the phenyl ring is the active chromophore. The subsequent thermal chemistry is more diverse, however, and probably includes disruption of the phenyl ring.[86]

Our results show the peptide group is a photochemically active chromophore, probably operating as an acceptor in electron-transfer reactions. While optical filtration by the atmosphere precludes direct absorption by the peptide group in photobiology, similar behavior in its ground state, as observed here with phenylalanyl peptides, may be promoted by excitation elsewhere,[21,87] and the possible implications for pathways in protein photodegradation[6,14] and in photobiological charge separation[7] merit some consideration. For example, present evidence of the ready participation of peptide groups in electron-transfer processes strengthens the possibility of their involvement as mediators in long-range electron transfer,[9] either as single components or in a chain.[88] The latter has been the subject of much speculation in both the excited- and ground-state redox chemistry of proteins,[8,10,12,89] and it has been investigated in model studies.[10,13,90] Preliminary results from the photolysis of triglycine indicate some sequential electron transfer does occur,[31] and its conformational dependence is currently under investigation.

Acknowledgment. We thank the Science and Engineering Research Council for mass spectrometry and high-field NMR services and Dr. P.G. Taylor for discussion on crystalline glycylglycine. Financial support from the Open University Research Committee and the Boots Company PLC is gratefully acknowledged.

Registry No. 3a, 60-35-5; **3b**, 79-05-0; **3c**, 541-46-8; **3d**, 102-93-2; **4a**, 625-51-4; **4b**, 7208-95-9; **4c**, 131213-42-8; **4d**, 123974-35-6; **5a**, 543-24-8; **5b**, 21709-90-0; **5c**, 16284-60-9; **5d**, 56613-60-6; **6a**, 3852-14-0; **6b**, 13025-15-5; **6c**, 131213-47-3; **7a**, 131213-39-3; **8a**, 22356-89-4; **8b**, 70875-70-6; **8c**, 87105-26-8; **8d**, 35373-92-3; **8e**, 52060-82-9; **9a**, 5663-60-5; *meso*-**9b**, 131320-19-9; (±)-**9b**, 131320-20-2; **9d**, 102036-11-3; **9e**, 54985-58-9; **10a**, 131213-40-6; **10b**, 131213-41-7; **10c**, 131213-43-9; **11**, 131213-44-0; **12**, 131213-45-1; **13a**, 112471-80-4; **13b**, 112471-79-1; Gly-Gly, 556-50-3; DL-Ala-Gly, 1188-01-8; Val-Gly, 686-43-1; Pro-Gly, 2578-57-6; Phe-Gly, 721-90-4; Gly-Phe, 3321-03-7; Pro-Phe, 13589-02-1; Phe-Pro, 7669-65-0; Gly, 56-40-6; Phe, 63-91-2; Gly-$NHCH_2CH_2Ph$, 62885-88-5; Cbz-Gly-ONp, 1738-86-9; Cbz-Phe-ONp, 2578-84-9; AcNHMe, 79-16-3; $(AcNHCH_2)_2$, 871-78-3; PhMe, 108-88-3; NH_3, 7664-41-7; CO_2, 124-38-9; $(CbzNHCH_2CONHCH_2)_2$, 73519-41-2; $H_2NCOCH_2CHMe_2$, 541-46-8; 2-piperidone, 675-20-7; 3-benzylpiperazine, 84477-71-4; (*S*)-3-benzylpiperazine-2,5-dione, 10125-07-2.

(85) Richer, G.; Sandorfy, C.; Naseimento, M. A. C. *J. Electron Spectrosc. Relat. Phenom.* **1984**, *34*, 327–335.

(86) Bazin, M.; Hasselmann, C.; Laustriat, G.; Santus, R.; Walrant, P. *Chem. Phys. Lett.* **1975**, *36*, 505–508.

(87) Kayushin, L. P.; Azizova, O. A.; Sud'bina, E. N. *Stud. Biophys.* **1975**, *49*, 199–214.

(88) Miller, J. R. *Nouv. J. Chim.* **1987**, *11*, 83–89.

(89) (a) Pullman, B. *Electronic Aspects of Biochemistry*; Academic Press: New York, 1964. (b) Bent, D. V.; Hayon, E. *J. Am. Chem. Soc.* **1975**, *97*, 2612–2619. (c) Szent-Gyorgyi, A. *The Living State and Cancer*; Dekker: New York, 1978. (d) Prutz, W. A.; Land, E. J.; Sloper, R. W. *J. Chem. Soc., Faraday Trans. 1* **1981**, *77*, 281–292. (e) Petrov, E. G. *Stud. Biophys.* **1983**, *96*, 237–240.

(90) (a) Isied, S. S.; Vassilian, A. *J. Am. Chem. Soc.* **1984**, *106*, 1726–1732. (b) Schanze, K. S.; Sauer, K. *J. Am. Chem. Soc.* **1988**, *110*, 1180–1186. Schanze, K. S.; Cabana, L. A. *J. Phys. Chem.* **1990**, *94*, 2740–2743.